ChemMedChem

Research Article
doi.org/10.1002/cmdc.202300160

Chemistry Europe
European Chemical Societies Publishing

www.chemmedchem.org

# Subnanomolar Cathepsin S Inhibitors with High Selectivity: Optimizing Covalent Reversible α-Fluorovinylsulfones and α-Sulfonates as Potential Immunomodulators in Cancer

Natalie Fuchs[+],[a] Mergim Meta[+],[a] Bellinda Lantzberg,[b] Matthias Bros,[c] Seah Ling Kuan,[b] Tanja Weil,[b] and Tanja Schirmeister*[a]

The cysteine protease cathepsin S (CatS) is overexpressed in many tumors. It is known to be involved in tumor progression as well as antigen processing in antigen-presenting cells (APC). Recent evidence suggests that silencing CatS improves the anti-tumor immune response in several cancers. Therefore, CatS is an interesting target to modulate the immune response in these diseases. Here, we present a series of covalent-reversible CatS inhibitors based on the $\alpha$-fluorovinylsulfone and -sulfonate warheads. We optimized two lead structures by molecular docking approaches, resulting in 22 final compounds which were evaluated in fluorometric enzyme assays for CatS inhibition and for selectivity towards the off-targets CatB and CatL. The most potent inhibitor in the series has subnanomolar affinity ($K_i = 0.08$ nM) and more than 100,000-fold selectivity towards cathepsins B and L. These new reversible and non-cytotoxic inhibitors could serve as interesting leads to develop new immunomodulators in cancer therapy.

## Introduction

Cysteine cathepsins are ubiquitous papain-like proteases, in mammalians mainly located in the lysosome, involved in extracellular matrix degradation and intracellular protein processing.[1] They have various functions in cells and, above all, share a high structural similarity.[2] However, cathepsin S (CatS) differs from other cysteine cathepsins in its stability at neutral pH and its limited tissue distribution (mainly in antigen-presenting cells, e.g. macrophages).[3,4] CatS is known to be overexpressed in many tumors (e.g., follicular lymphoma, breast, gastric, colon, pancreatic cancer).[5–8] To date, various mechanisms how CatS is involved in tumor progression are known. For example, CatS is known to turn over extracellular matrix proteins and to drive tumor angiogenesis.[7,9] Additionally, Riese and co-workers showed that CatS regulates antigen processing and presentation in antigen-presenting cells (APC).[10–15] With this important role in immune cells, cathepsin S intervenes in the body's immune response also to tumors. It shifts MHC-II expression to MHC–I, resulting in a favored activation of CD4+ T cells (e.g., regulatory T cells) over cytotoxic CD8+ T cells.[5,6,16] Jakoš and co-workers and Wilkinson and co-workers also stated that CatS polarizes APCs from M1 to M2 phenotype that is associated with tumor progression, supporting the proliferation of myeloid-derived suppressor cells (MDSC) and tumor-associated macrophages.[9,16] This shift results in a suppressed T cell-induced immune response.[17–19] Data from murine models also indicates that CatS inhibition reduces the overall T cell immunity in healthy mice but enhances the CD8+ T cell immunity in mice with cancer.[20] Cytotoxic CD8+ T cells can attack tumor cells and thus lead to tumor volume reduction.[20] Experiments with small-interfering RNA (siRNA) targeting CatS mRNA and thus, reducing CatS expression, resulted in tumor volume and invasion reduction as well as increased apoptosis and attenuated angiogenesis.[21,22] Burden and co-workers used inhibitory CatS antibodies and observed an increased effect of chemotherapeutics plus a significant tumor growth limitation.[23,24] Furthermore, CatS overexpression occurs in follicular lymphoma including the expression of an overactive mutant (Y132D) with enhanced auto-activation.[5] Knocking down the protease leads to an improved immune response towards lymphoma cells.[6] Overall, CatS is an interesting new target to enhance anti-tumor immunogenicity and thus, stop tumor growth, especially in case of resistances to current tumor immunotherapies.[6,10,25,26] Figure 1 summarizes the mentioned effects of CatS in the tumor microenvironment (TME).

CatS is a papain-like protease expressed as an inactive zymogen.[27,28] After cleaving off the propeptide, the mature enzyme consists of 217 residues and a catalytic dyad (Cys25, His164) in the active site.[3,4,29] Despite the high structural similarity to other human cathepsins, there are various residues

[a] N. Fuchs,[+] M. Meta,[+] Prof. Dr. T. Schirmeister
Institute of Pharmaceutical and Biomedical Sciences (IPBS)
Johannes Gutenberg University Mainz
Staudingerweg 5, 55128 Mainz (Germany)
E-mail: schirmei@uni-mainz.de
[b] B. Lantzberg, Dr. S. Ling Kuan, Prof. Dr. T. Weil
Max Planck Institute for Polymer Research
Ackermannweg 10, 55128 Mainz (Germany)
[c] Dr. M. Bros
Department of Dermatology, University Medical Center Mainz
Langenbeckstr. 1, 55131 Mainz (Germany)
[+] These authors contributed equally to this work.

Supporting information for this article is available on the WWW under https://doi.org/10.1002/cmdc.202300160

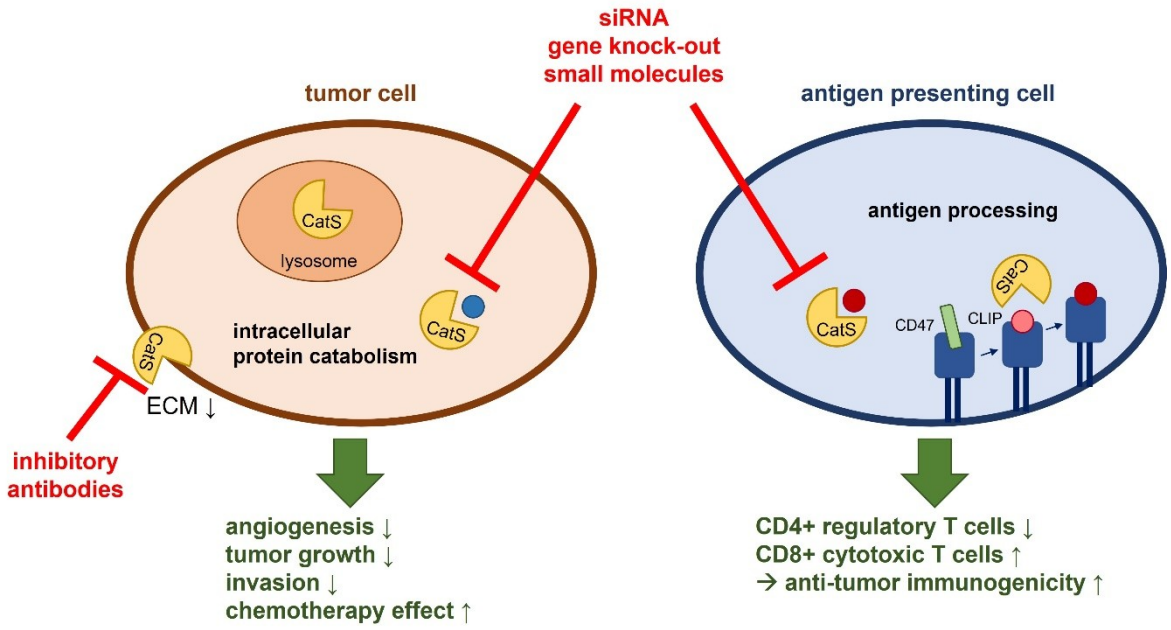


**Figure 1.** Cathepsin S inhibition affects tumor cells and antigen presenting cells (APC). CLIP = Class II-associated invariant chain peptide.

in the S1′ to S3 subsites that differ and can be addressed to gain selectivity.[4,29] The first selective CatS inhibitors were published in the early 2000s based on a publication by Pauly et al. that described the binding site and especially the differences towards other cysteine cathepsins.[1,29]

The S2 subsite contains a flexible Phe211 residue that can flip and open up to Phe70 from the S3 site, creating space for bulkier residues in S2. Furthermore, it allows ligand π-stacking with these Phe residues.[1,30] During the last 20 years, many cathepsin S inhibitors have been developed, including non-covalent as well as covalent ones (e.g. vinylsulfones, nitriles, aldehydes).[1,30–38] One nitrile-based inhibitor has already been tested *in vivo*. The compound led to significant reduction of tumor volume in murine models.[39] The structures of three advanced CatS inhibitors are summarized in Scheme 1.[30,40,41]

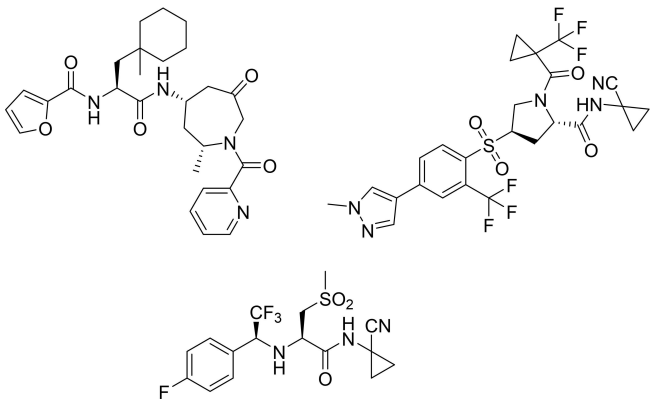

**Scheme 1.** Structures of three advanced published CatS inhibitors.[30,40,41]

Here, we focus on developing new selective cathepsin S inhibitors based on the structure of the well-known pan-cathepsin inhibitor K11777. This compound with an electrophilic vinylsulfone warhead is known to be a covalent irreversible cathepsin inhibitor (Figure 2).

The active site cysteine undergoes a Michael-type addition and cannot dissociate from the inhibitor after the covalent bond formation. Since irreversible inhibition has several drawbacks, e.g., off-target effects, toxicity, haptenization, we have recently developed modified K11777 derivatives by introducing a fluorine atom at the α-position of the vinylsulfone double bond.[42–44] The generated α-fluorovinylsulfone (**1 a**) undergoes a reversible Michael-type addition with thiols (Figure 2).[45] With this reversibility we maintain the benefits of covalent inhibition, e.g., longer residence times, higher potency, thus possible dosage reduction, and a lower pharmacokinetic sensitivity, without the drawbacks of irreversible inhibition mentioned above.[46–48]

Our most recent findings suggest that modifying the warhead from an α-fluorovinylsulfone (**1 a**) to an α-fluorovinylsulfonate (**1 b**) results in slowly reversible cathepsin inhibitors, further prolonging the target residence time (Figure 2).[49]

Since covalent-reversible inhibition has many benefits, we chose previously described fluorinated derivatives from Schirmeister et al. and Jung, Fuchs et al. as initial starting structures (**1 a**, **1 b**) for the development of new CatS inhibitors.[45,49] Results of molecular docking studies combined with literature-known motifs resulted in 22 new compounds (Figure 3) that were tested in fluorometric enzyme assays against cathepsins S, B, and L. We evaluated their potency and selectivity profiles in a structure-activity relationship study backed up by molecular docking results. Finally, their cytotoxicities against the breast

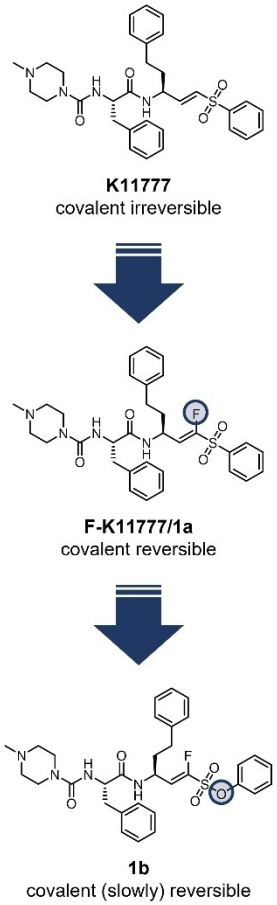


**Figure 2.** Reversible K11777 derivatives as lead structures for CatS inhibitor development.

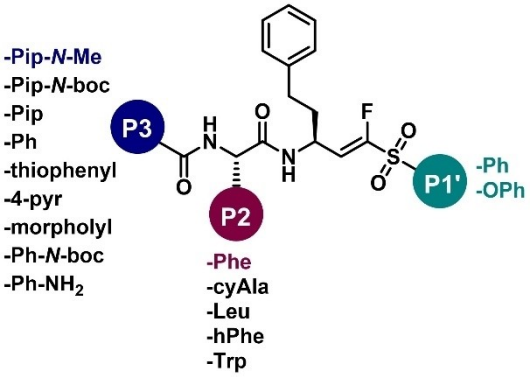


**Figure 3.** SAR variations for compounds **1a** (P1′=Ph) and **1b** (P1′=OPh). Residues of initial leads are highlighted.

cancer cell line MDA-MB-231 and murine bone marrow-derived dendritic cells were tested in cell viability assays.

## Results and Discussion

Starting from lead structures **1a** and **1b**,[45,49] we prepared 22 new compounds (**2a**–**6c**, Scheme 2).

The compounds differ in their P2 and P3 positions (Scheme 2). They contain morpholine (**2c**, **3c**, **6c**), piperazine (Pip, **2b**, **3b**), *N*-boc-piperazine (Pip-*N*-boc, **2a**, **3a**), pyridine (**2d**, **3d**, **4a**–**5d**), thiophene (**2e**, **3e**) or aniline (Ph–$NH_2$, **6b**) in the P3 position and hPhe (**4c**, **5c**), cyAla (**4a**, **5a**, **6a**–**c**), Leu (**4b**, **5b**) and Trp (**4d**, **5d**; all with (*S*)-configured stereo center) in the P2 position. These latter residues were previously described to improve the binding affinity in CatS inhibitors.[34] For the covalently reacting warhead functionality, we prepared $\alpha$-fluorovinylsulfones and the corresponding $\alpha$-fluorovinylsulfonates occupying the P1 position.

### Chemistry

The synthesis route allowed many combinations of the two warhead variations with various dipeptides, resulting in the final inhibitors **1a**–**6c**.

### Warhead preparation

To prepare the warhead, we first synthesized fluorinated phosphonates **11** and **12** (Scheme 3) as previously published.[49] To synthesize aldehyde **14**, we prepared the Weinreb amide **13**

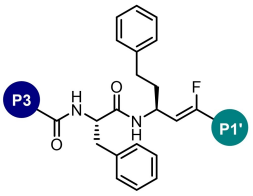


**2a**: P1' = $SO_2Ph$, P3 = Pip-*N*-boc
**2b**: P1' = $SO_2Ph$, P3 = Pip
**2c**: P1' = $SO_2Ph$, P3 = morpholyl
**2d**: P1' = $SO_2Ph$, P3 = 4-pyridyl
**2e**: P1' = $SO_2Ph$, P3 = 3-thiophenyl
**3a**: P1' = $SO_3Ph$, P3 = Pip-*N*-boc
**3b**: P1' = $SO_3Ph$, P3 = Pip
**3c**: P1' = $SO_3Ph$, P3 = morpholyl
**3d**: P1' = $SO_3Ph$, P3 = 4-pyridyl
**3e**: P1' = $SO_3Ph$, P3 = 3-thiophenyl
**3f**: P1' = $SO_3Ph$, P3 = phenyl

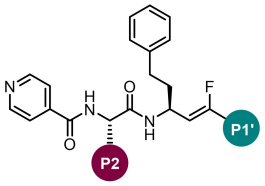


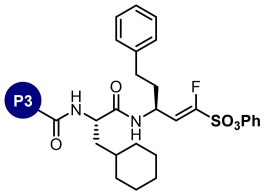


**4a**: P1' = $SO_2Ph$, P2 = cyAla
**4b**: P1' = $SO_2Ph$, P2 = Leu
**4c**: P1' = $SO_2Ph$, P2 = hPhe
**4d**: P1' = $SO_2Ph$, P2 = Trp
**5a**: P1' = $SO_3Ph$, P2 = cyAla
**5b**: P1' = $SO_3Ph$, P2 = Leu
**5c**: P1' = $SO_3Ph$, P2 = hPhe
**5d**: P1' = $SO_3Ph$, P2 = Trp

**6a**: P3 = Ph-*N*-boc
**6b**: P3 = Ph-$NH_2$
**6c**: P3 = morpholyl

**Scheme 2.** Optimized cathepsin S inhibitors with variations in P1′, P2 and P3.

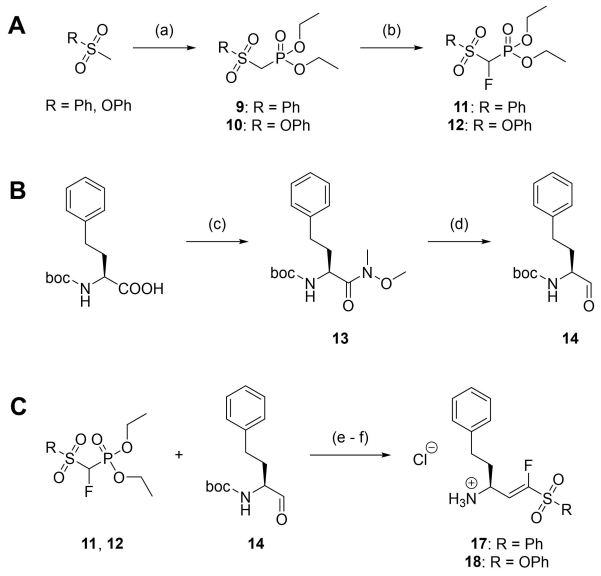


**Scheme 3.** (**A**) Phosphonate preparation (**9**–**12**). (a) KHMDS/*n*-BuLi, DECP; THF; −78/0 °C; 3 h; 43–82 %. (b) LHMDS, Selectfluor; THF/DMF; −78 °C–0 °C; 4 h; 45–46 %. (**B**) Aldehyde preparation (**13**–**14**). (c) *N,O*-dimethyl hydroxylamine, HOBt, TBTU, DIPEA; DCM; 0 °C – rt; 12 h; 100 %. (d) $LiAlH_4$; diethyl ether; 0 °C; 2 h; 99 %. (**C**) HWE olefination (**15**–**16**) and boc deprotection (**17**–**18**). (e) LHMDS; THF; −78 °C; 4 h; 46–59 %. (f) 4 M HCl; dioxane; rt; 2 h; 88–95 %.

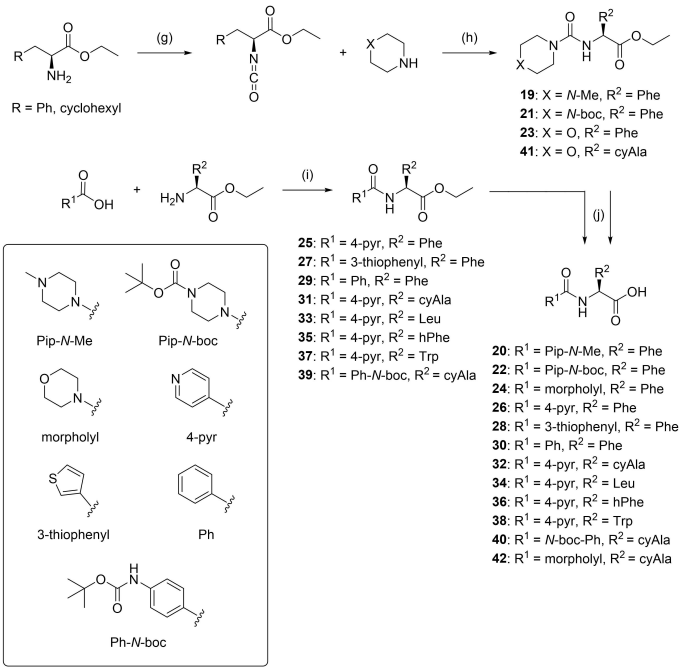


**Scheme 4.** Synthesis of dipeptides **20**–**42**. (g) Triphosgene, $NaHCO_3$; DCM/toluene; 0 °C; 3 h; 64 %. (h) DIPEA; THF; 0 °C – rt; 12–24 h; 84–100 %. (i) HOBt, TBTU, DIPEA; DCM; 0 °C – rt; 12–24 h; 67–100 %. (j) LiOH × 1 $H_2O$; THF/H2O; rt; 12–24 h; 44–100 %.

of boc-homophenylalanine which was subsequently reduced to **14** using $LiAlH_4$ (Scheme 2). Aldehyde **14** and phosphonates **11** or **12** then reacted in a Horner-Wadsworth-Emmons olefination, providing fluorovinylsulfone **15** and fluorovinylsulfonate **16**. Boc-deprotection with HCl in dioxane resulted in **17**/**18** (Scheme 3).

### Dipeptide synthesis

For ester-protected dipeptides **19**, **21**, **23** and **41**, we prepared isocyanates which then reacted with piperazine derivatives or morpholine. We synthesized the other ester-protected dipeptides using standard amide coupling reactions. The cleavage of the ester moieties by hydrolysis under basic conditions gave access to the final dipeptides **20**–**42** (Scheme 4).

### Amide couplings

Warheads **17** or **18** were coupled with dipeptides **20**–**42** in standard amide coupling reactions (Scheme 5). The resulting inhibitors **1a**–**6c** were purified by HPLC (>95 % purity in all cases). For some compounds (**4c**, **6a**, **6b**) the formation of diastereomers could not be avoided, but the (*E*)-configurations of the isolated, purified and tested inhibitors were confirmed in all cases using the coupling constants in the NMR.

### Fluorometric enzyme assays

The synthesized compounds' inhibitory activities against CatS and the off-targets CatB and CatL were tested using well-known fluorometric enzyme assays (Table 1).[50] The inhibitors were initially screened at different concentrations (20 μM, 1 μM) followed by $IC_{50}/K_i$ value determination if >50 % inhibition at 20 μM. For more information regarding assay procedures and calculations of inhibition constants see 'Fluorometric enzyme assay' in the Experimental Section.

We started by varying the P3 position of lead compounds **1a** and **1b** (Figure 3) and prepared two compound sets, namely the corresponding fluorovinylsulfones/-sulfonates (**2a**–**6c**), and evaluated their inhibitory activities and selectivities (Table 1). We generally observed all $\alpha$-fluorovinylsulfonates (**3a**–**3f** & **5a**–**5c**) to be more potent cathepsin S inhibitors than the corresponding $\alpha$-fluorovinylsulfones (**2a**–**2e** & **4a**–**4d**) which already improves their selectivity towards CatB and CatL (Table 1).

We noted a good inhibition for compound **2c** ($K_i$ = 40 nM), but a low selectivity (only 9.3-fold vs. CatB and 4.5-fold vs. CatL). The corresponding fluorovinylsulfonate **3c** has a 40-fold increased inhibitory activity ($K_i$ = 0.9 nM), also resulting in higher selectivity towards other cathepsins (1,333-fold vs. CatB, 333-fold vs. CatL).

Next, we altered the P2 position while maintaining a 4-pyridyl residue in P3, an effective strategy to achieve the most potent and selective P2 residues. The 4-pyr moiety was among

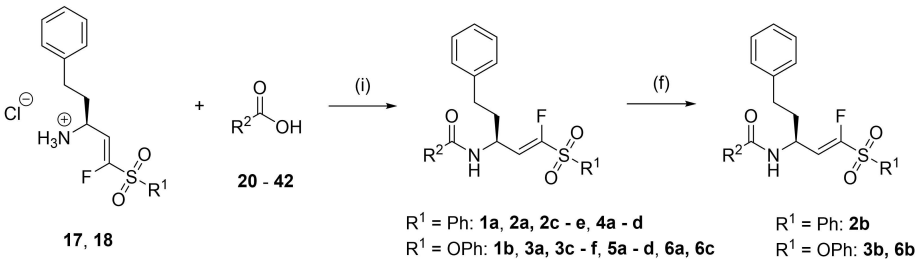


**Scheme 5.** Amide coupling reactions of warheads and dipeptides resulting in the final inhibitors **1a**–**6c**. (i) HOBt, TBTU or HATU, DIPEA; DCM or DCM/DMF; 0 °C – rt; 12–24 h; 11–65 %. (f) 4 M HCl; dioxane; rt; 2 h; 74–96 %.

**Table 1.** Enzyme assay results for compounds **2a**–**6c** compared with **1a** and **1b**.

| Compd | P1′ | P2 | P3 | Ki CatS [μM] | Ki CatB [μM] | SI CatB/CatS | Ki CatL [μM] | SI CatL/CatS |
|---|---|---|---|---|---|---|---|---|
| **1a** | Ph | Phe | Pip-*N*-Me | 1.2 ± 0.28 | 0.47[a] | 0.39 | 0.023[a] | 0.02 |
| **1b** | OPh | Phe | Pip-*N*-Me | 0.010 ± 0.002[c] | 0.26 ± 0.038 | 26 | 0.024 ± 0.003 | 2.4 |
| **2a** | Ph | Phe | Pip-*N*-boc | 0.14 ± 0.056 | > 12 | > 86 | > 10 | > 71 |
| **2b** | Ph | Phe | Pip | 1.3 ± 0.37 | 0.66 ± 0.084 | 0.51 | 0.79 ± 0.21 | 0.61 |
| **2c** | Ph | Phe | morpholyl | 0.040 ± 0.004 | 0.37 ± 0.096 | 9.3 | 0.18 ± 0.043 | 4.5 |
| **2d** | Ph | Phe | 4-pyridyl | 0.10 ± 0.012 | 3.1[a] | 31 | 0.11[a] | 1.1 |
| **2e** | Ph | Phe | 3-thiophenyl | 0.057 ± 0.008 | 1.1 ± 0.38 | 19 | 0.56 ± 0.097 | 9.8 |
| **3a** | OPh | Phe | Pip-*N*-boc | 0.0085 ± 0.0045[c] | > 12 | > 1,400 | > 10 | > 1,100 |
| **3b** | OPh | Phe | Pip | 0.0057 ± 0.0023[c] | 0.84 ± 0.20 | 147 | 0.087 ± 0.010 | 15 |
| **3c** | OPh | Phe | morpholyl | 0.0009 ± 0.0005[c] | 1.2 ± 0.20 | 1,333 | 0.30 ± 0.014 | 333 |
| **3d** | OPh | Phe | 4-pyridyl | 0.0008 ± 0.0004[c] | 1.7[b] | 85 | 0.26[b] | 13 |
| **3e** | OPh | Phe | 3-thiophenyl | 0.011 ± 0.0039[c] | 4.0 ± 0.98 | 363 | 0.97 ± 0.059 | 88 |
| **3f** | OPh | Phe | Ph | 0.0073 ± 0.0018[c] | > 12 | > 1,600 | 0.19 ± 0.16 | 26 |
| **4a** | Ph | cyAla | 4-pyridyl | 0.0059 ± 0.0008 | > 15 | > 2,500 | > 10 | > 1,700 |
| **4b** | Ph | Leu | 4-pyridyl | 0.11 ± 0.011 | > 12 | > 110 | 0.56 ± 0.11 | 5.1 |
| **4c** | Ph | hPhe | 4-pyridyl | 0.17 ± 0.0033 | > 15 | > 88 | > 10 | > 59 |
| **4d** | Ph | Trp | 4-pyridyl | 0.32 ± 0.043 | > 12 | > 38 | 2.3 ± 0.61 | 7.2 |
| **5a** | OPh | cyAla | 4-pyridyl | 0.0079 ± 0.0038[c] | > 15 | > 1,900 | > 10 | > 1,300 |
| **5b** | OPh | Leu | 4-pyridyl | 0.035 ± 0.012[c] | > 12 | > 340 | > 10 | > 290 |
| **5c** | OPh | hPhe | 4-pyridyl | 0.24 ± 0.11[c] | > 12 | > 50 | > 10 | > 42 |
| **5d** | OPh | Trp | 4-pyridyl | 0.018 ± 0.0023[c] | 1.7 ± 0.17 | 94 | 0.66 ± 0.076 | 37 |
| **6a** | OPh | cyAla | Ph-*N*-boc | 0.0059 ± 0.0018[c] | > 12 | > 2,000 | > 10 | > 1,700 |
| **6b** | OPh | cyAla | Ph-$NH_2$ | 0.0090 ± 0.0017[c] | > 12 | > 1,330 | > 10 | > 1,100 |
| **6c** | OPh | cyAla | morpholyl | 0.00009 ± 0.00002[c] | > 12 | > 150,000 | > 10 | > 125,000 |

[a] See Schirmeister et al.[45] [b] See Jung, Fuchs, et al.[49] [c] Time-dependent inhibition.

the top two residues in P3 regarding potency and selectivity with a better synthetic accessibility than morpholyl.[35]

Here, we also prepared corresponding $\alpha$-fluorovinylsulfones/-sulfonates (**4a**–**5d**) and determined their inhibitory activities and selectivity profiles (Table 1). The cyAla residue in P2 seems to be the most favorable, with $K_i$ values in the low nanomolar range (5.9–7.9 nM) for both warheads (**4a**, **5a**, see Table 1). The resulting selectivity towards CatB and CatL is > 1,000-fold for both compounds and enzymes. Leucin in P2 combined with an $\alpha$-fluorovinylsulfonate (**5b**) also shows good CatS inhibition ($K_i$ = 35 nM) and high selectivity, but lacks selectivity compared to **5a** with cyAla in P2. Homophenylalanine and tryptophane are not suitable as they lack affinity and selectivity compared to the most favorable compounds.

Based on the results from these first optimizations, we prepared three additional compounds (**6a**–**6c**) with cyAla in P2 and modifications in P3. For future attachments of our inhibitors onto nanodelivery systems via various linkers, we chose to introduce an amino-substituted phenyl ring in the P3 position (**6b**). We also tested the *N*-boc protected intermediate **6a**. Since we had found the morpholyl substituted compounds **2c**, **3c** to be very potent, with $K_i$ values of 0.9 nM (**3c**) and 40 nM (**2c**) respectively, we prepared a final inhibitor combining the favorable cyAla residue in P2 with the morpholyl moiety in P3 (**6c**). The results shown in Table 1 reveal that all three moieties are suitable for the P3 position with $K_i$ values in the low nanomolar or even subnanomolar range and high selectivities towards cathepsins B and L. However, it should be noted that combining suitable residues in P2, P3 and the most potent warhead is essential to achieve a highly active and selective inhibitor. Compound **6c** (morpholyl in P3, cyAla in P2, F-vinylsulfonate warhead) with a $K_i$ value around 90 pM and more than 100,000-fold selectivity towards the other two cathepsins is the most potent and selective inhibitor of the series.

To verify the extraordinarily high inhibition potency of **6c**, we also used an alternative substrate (*Z*-Phe-Arg-AMC) and

repeated the inhibition experiments, resulting in a similar $K_i$ (120 pM, see Figure 5 and Fluorometric enzyme assay).

Generally, the progress curves for α-fluorovinylsulfones are linear, indicating that the inhibition is not time-dependent (Figure 4). For the α-fluorovinylsulfonates, we observed time-dependent inhibition (Figure 5) with biphasic binding behavior as we have reported previously for α-fluorovinylsulfonate inhibitors of the cysteine protease rhodesain.[49] Thus, we also determined further inhibition constants, such as $k_3$, $k_4$ and $K_i$* (dissociation constant of final covalent complex) using the slow-binding equation for these compounds [**1b**, **3a–f**, **5a–6c**, Table 2, and Equation (1), which depicts enzyme-inhibitor complex formation and the relevant constants].[51]

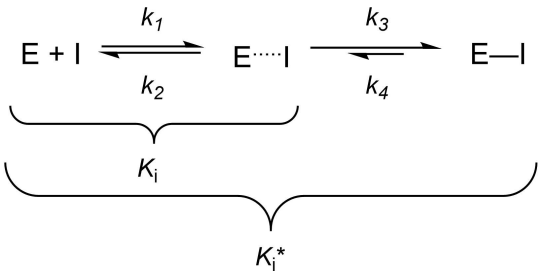


(1)

We found the rate constant of the dissociation of the final complex ($k_4$) to be significantly lower than the association rate constant ($k_3$) for all time-dependent compounds (Table 2), suggesting tight-binding behavior. The dissociation constants of the final covalent complexes ($K_i$*) are in the low nanomolar

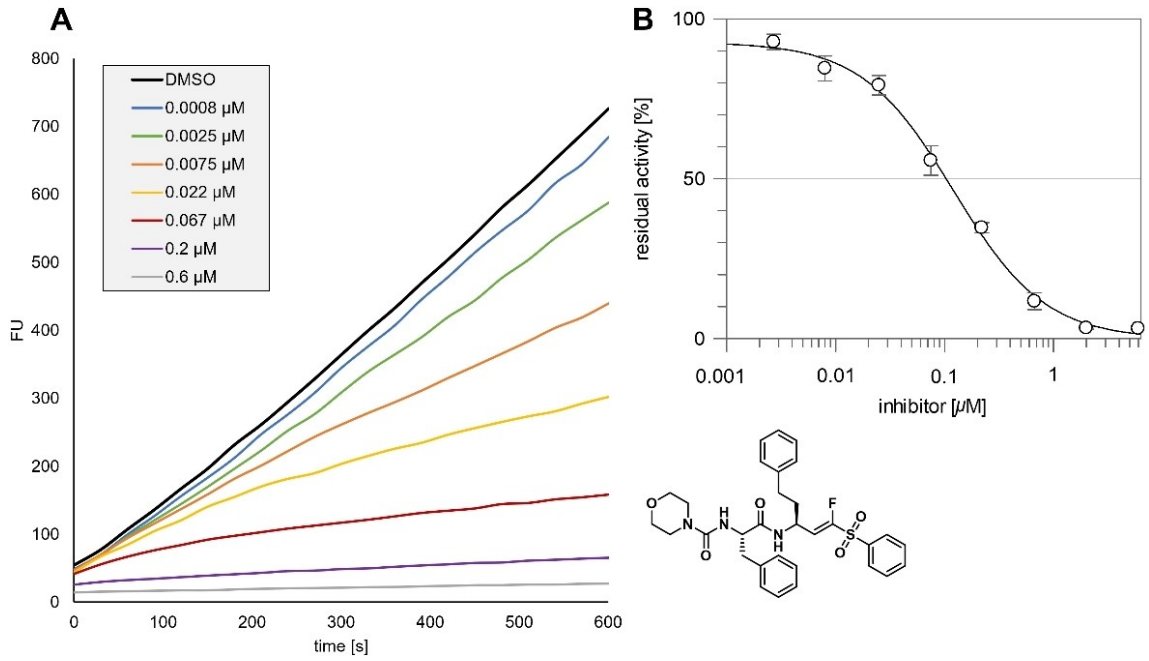


**Figure 4.** Assay results for **2c** (bottom right). (**A**) Fluorescence-time plot for **2c** vs. CatS with different inhibitor concentrations [µM] showing linear progress curves. (**B**) Residual enzyme activity [%] vs. inhibitor concentration [µM] for $IC_{50}$ calculation. $K_i$ value was calculated using the Cheng-Prusoff equation.[51]

**Table 2.** Inhibition data and kinetic constants for time-dependent CatS inhibitors.[a]

| Compd | P2 | P3 | Ki [µM] | k3 [s-1] | k4 [s-1] | Ki* [µM] |
|---|---|---|---|---|---|---|
| **1b** | Phe | Pip-*N*-Me | 0.010 ± 0.002 | 0.0015 | 0.0002 | 0.0012 |
| **3a** | Phe | Pip-*N*-boc | 0.0085 ± 0.0045 | 0.0024 | 0.0004 | 0.0012 |
| **3b** | Phe | Pip | 0.0057 ± 0.0023 | 0.0020 | 0.0004 | 0.0010 |
| **3c** | Phe | Morpholyl | 0.0009 ± 0.0005 | 0.0021 | 0.0003 | 0.00011 |
| **3d** | Phe | 4-pyridyl | 0.0008 ± 0.0004 | 0.0012 | 0.0004 | 0.00020 |
| **3e** | Phe | 3-thiophenyl | 0.011 ± 0.0039 | 0.0016 | 0.0002 | 0.0012 |
| **3f** | Phe | Ph | 0.0073 ± 0.0018 | 0.0018 | 0.0003 | 0.0010 |
| **5a** | cyAla | 4-pyridyl | 0.0079 ± 0.0038 | 0.0015 | 0.0003 | 0.0013 |
| **5b** | Leu | 4-pyridyl | 0.035 ± 0.012 | 0.0016 | 0.0003 | 0.0055 |
| **5c** | hPhe | 4-pyridyl | 0.24 ± 0.11 | 0.0017 | 0.0002 | 0.025 |
| **5d** | Trp | 4-pyridyl | 0.018 ± 0.0023 | 0.0022 | 0.0002 | 0.0015 |
| **6a** | cyAla | Ph-*N*-boc | 0.0059 ± 0.0018 | 0.0019 | 0.0002 | 0.00056 |
| **6b** | cyAla | Ph-$NH_2$ | 0.0090 ± 0.0017 | 0.0007 | 0.0001 | 0.00038 |
| **6c** | cyAla | morpholyl | 0.00009 ± 0.00002 | 0.0017 | 0.0002 | 0.00001 |

[a] $k_3$, $k_4$ and $K_i$* calculated with the slow-binding equation.[52]

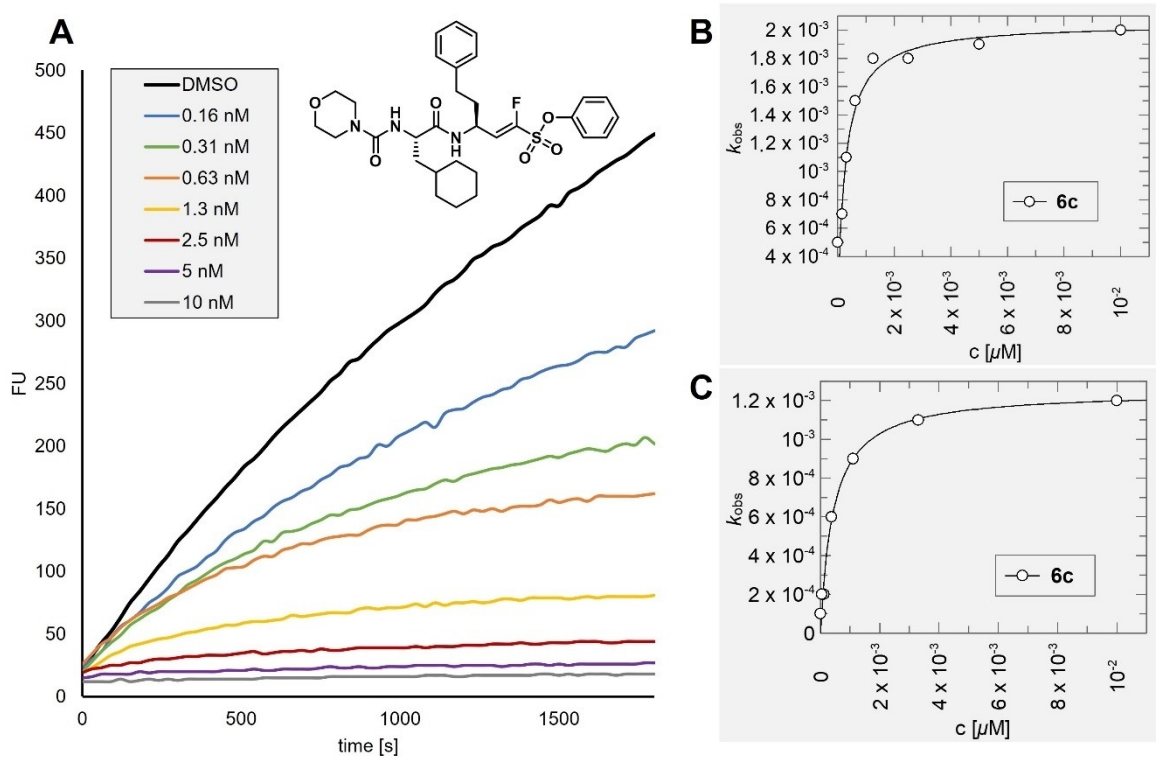


**Figure 5.** Assay results for **6c** (bottom right). (**A**) Fluorescence-time plot for **6c** vs. CatS with different inhibitor concentrations [nM] showing a biphasic behavior, thus a time-dependent inhibition mode. Substrate: *Z*-Val-Val-Arg-AMC. (**B**) $k_{obs}$ [$s^{-1}$] vs. inhibitor concentration [μM] plots resulting from assays with substrate *Z*-Val-Val-Arg-AMC for $K_i$ calculation using the slow-binding equation.[52] (**C**) $k_{obs}$ [$s^{-1}$] vs. Inhibitor concentration [μM] plots resulting from assays with substrate *Z*-Phe-Arg-AMC for $K_i$ calculation using the slow-binding equation.[52]

to subnanomolar range proving the very tight binding of the inhibitors.

### Dilution assay

With dilution assays, we proved that the inhibitors are reversible as expected from our previous experiences with such compounds.[49] For the experiments, two compounds (F-vinylsulfonate **3c**, F-vinylsulfone **4a**) were incubated with cathepsin S, followed by 100-fold dilution with substrate-containing assay buffer. In case of reversible inhibition, the enzyme activity should recover. Furthermore, we used the pan-cathepsin inhibitor K11777 as an irreversible control.[53]

Figure 6 shows that enzyme activity can be recovered for F-vinylsulfones and -sulfonates, suggesting reversible inhibition as anticipated.

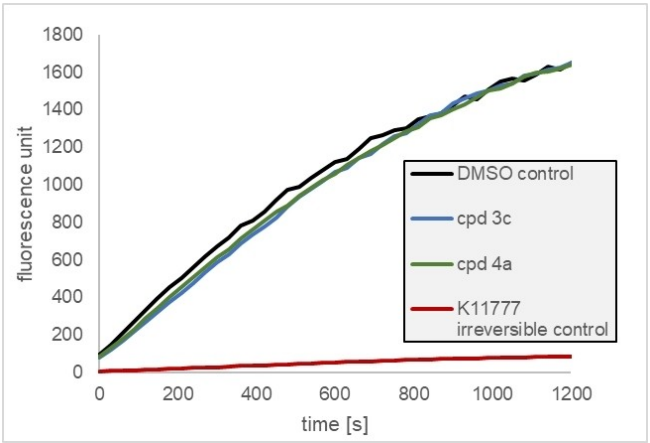


**Figure 6.** Dilution assays. DMSO as control (black) and **K11777** as irreversible control (red). Incubation of CatS with compounds **3c** (F-vinylsulfonate, blue) and **4a** (F-vinylsulfone, green) followed by 100-fold dilution results in an enzyme activity recovery.

### SAR discussion

Comparing the $K_i$ values of the lead compounds F-vinylsulfone **1a** ($K_i$ = 1.2 μM) and F-vinylsulfonate **1b** ($K_i$ = 0.010 μM) with P3 substituted inhibitors **2a**–**2e** and **3a**–**3f** shows significantly enhanced affinity towards the target enzyme CatS in all cases except for piperidyl substituted vinylsulfone **2b** ($K_i$ = 1.3 μM) and 3-thiophenyl substituted vinylsulfonate **3e** ($K_i$ = 0.011 μM). The non-covalent docking results show scores in the same range or even higher compared to the leads **1a** & **1b**. For compound **3f** the predicted score for the stability of the covalent complex is even higher compared to the lead compounds (see Table B, Supporting Information). Additionally,

the selectivities for CatS increased significantly towards CatB for all P3 modified compounds (**2a**–**3f**) by up to 220-fold for inhibitor **2a** vs **1a**. The selectivity towards CatL also improved in all cases (**2a**–**3f**) from 0.02-fold for **1a** to >71-fold for **2a** (vinylsulfones) and from 2.4-fold for **1b** to >1,100-fold for **3a** (vinylsulfonates). Overall, the vinylsulfonate warhead resulted in more potent inhibitors as exemplified for compounds **2b** vs **3b**. Superposition of the covalent docking poses of both compounds revealed that the phenylalanine substituent of **3b** leads to a different orientation of the phenyl ring inside the S2 subpocket of the active site, where additional face to edge and face to face π-stacking interactions with Phe211 and Phe70 could be possible, possibly leading to tighter binding of **3b** compared to **2b** (Figure 7).

Replacing phenylalanine in P2 with four different amino acids while maintaining the 4-pyridyl substituent in P3 lead to the result that the cyAla-residue is best suited to address the S2 pocket of the enzyme with both warheads. This is highlighted by the increase in potency for the vinylsulfone-based inhibitor **4a** ($K_i$ = 0.006 μM) compared to **2d** ($K_i$ = 0.10 μM) and a better selectivity towards both off-targets (>2,500-fold vs CatB and >1,700-fold vs CatL). For the vinylsulfonate-based inhibitor series, the same exchange resulted in a potency drop of about 10-fold (**3d** vs **5a**) but a big jump in selectivity (>1,900-fold vs CatL and >1300-fold vs CatL) for inhibitor **5a**. This might be due to the $sp^3$-hybridization of the carbon atoms of the cyAla substituent, which better fills the S2 subpocket of CatS and presumably generates new non-polar interactions with the subpocket atoms compared to the $sp^2$-hybridized planar phenyl ring (Figure 8). The S2 pockets of both off-target cathepsins lack the depth for accepting bulky residues. Additionally, a water molecule present in the S2 pocket, could putatively be expelled by the hydrophobic cyAla residue and thus lead to a change in entropy and thereby have an impact on the binding free energy.

Combining the cyAla motif in P2 with morpholine in P3 and the vinylsulfonate warhead yielded the most potent inhibitor **6c**, with a $K_i$-value in the picomolar range and excellent selectivities over CatB (>150,000) and CatL (>125,000). Superposition of the non-covalent docking pose of **6c** with the covalent enzyme-inhibitor complex shows that all polar interactions between the non-covalently bond inhibitor and the enzyme should still be intact after the covalent bond formation (Figure 9). Compound **6c** also has one of the highest scores for the stability of the covalent enzyme inhibitor complex (Affinity △G, MOE-score = −6.0 kcal/mol) as well as the second highest HYDE-score of all inhibitors with −50 kJ/mol (Table B, Supporting Information).

The incorporation of an amine functionality in the P3 site for compound **6b** ($K_i$ = 9 nM) and its boc-protected intermediate **6a** ($K_i$ = 6 nM) did not deteriorate the affinity or the selectivity for the target enzyme (Table 1). Therefore, **6b** can be used in future studies with nanodelivery systems.

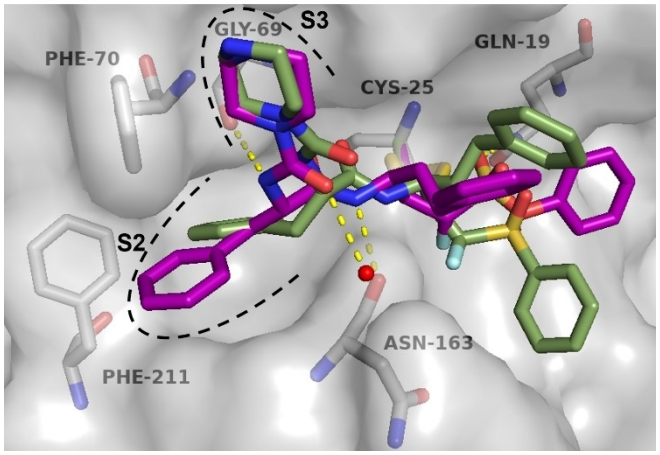


**Figure 7.** Superposition of the covalent docking poses of **2b** (smudge green carbon atoms) and **3b** (purple carbon atoms) inside the active site of CatS (pdb: 1NPZ). Polar interactions between **3b** and the enzyme are depicted as yellow dashed lines.

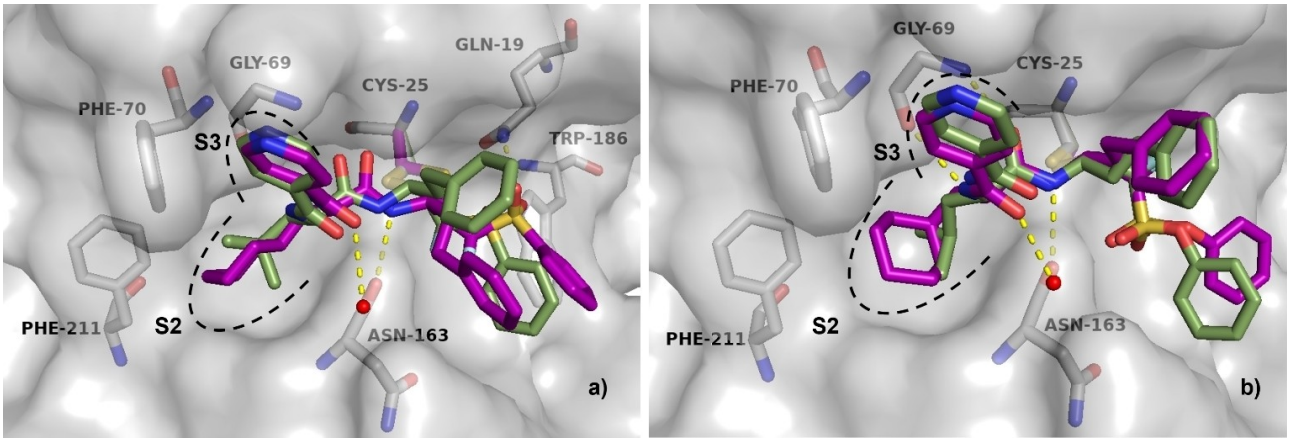


**Figure 8.** Predicted binding modes and non-covalent interactions (yellow dashed lines) of different inhibitors inside the CatS binding pocket (pdb: 1NPZ). (**A**) Superposition of the covalent docking poses of **4a** (purple carbon-atoms) & **4b** (smudge green carbon atoms). (**B**) Superposition of the covalent docking poses of **5a** (purple carbon-atoms) & **5b** (smudge green carbon atoms).

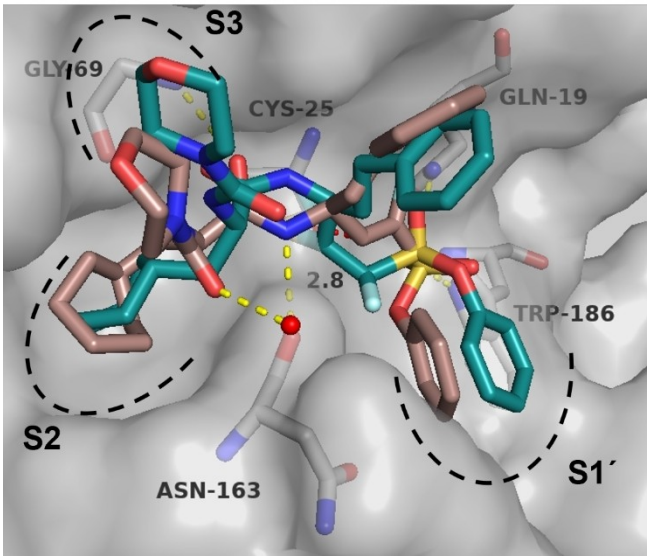


**Figure 9.** Superposition of the non-covalent docking pose of **6c** (darksalmon carbon atoms) and the covalent docking pose of **6c** (teal carbon atoms) inside the active site of CatS (pdb: 1NPZ). Polar interactions between the non-covalent pose of **6c** and the enzyme are depicted as yellow dashed lines. The distance between the electrophilic C-atom of **6c** and Cys25 is shown as red dashed line with the measured distance in Å.

### Cell viability

Selected compounds were tested in a CellTiter-Glo Luminescent Cell Viability assay to assess their cytotoxicity. We used MDA-MB-231 cells which are breast cancer cells that compensate the inhibition of CatS and other cathepsins. Therefore, only unspecific cytotoxic effects, that are not related to CatS inhibition, are detected.[54] We did not observe significant cytotoxicity (Figure 10) after 24 h treatment at concentrations >1,000-fold higher (20 μM) than the compounds' $K_i$ values in the low nanomolar range. Only compounds **5a** and **6b** exhibited low cytotoxic effects at the highest concentration applied (100 μM), which was >10,000-fold the compounds' $K_i$ values. In conclusion, the exemplarily selected compounds do not affect cell viability of MDA-MB-231 cells at their biologically active concentrations.

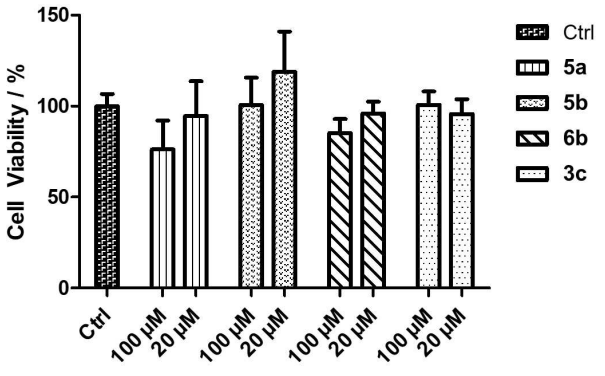


**Figure 10.** Cell viability of compounds **5a**, **5b**, **6b** and **3c**-treated MDA-MB-231 cells determined by CellTiter-Glo Luminescent Cell Viability Assay. Cells were treated for 24 h with each compound at two different concentrations, 100 μM or 20 μM, respectively. Significant cytotoxic effect was observed for MDA-MB-231 cells treated with **5a** and **6b** at 100 μM. All experiments were performed in quadruplicates and data are shown as mean ± SD from three independent experiments.

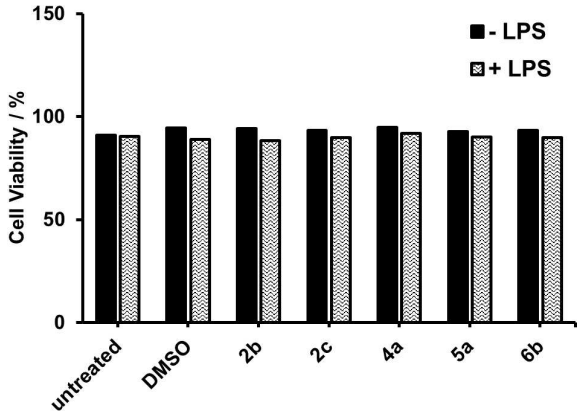


**Figure 11.** Cell viability of compounds **2b**, **2c**, **4a**, **5a**, and **6b**-treated murine CD11c$^+$ DC. Cells were treated for 24 h with each compound at 1 μM concentration. No significant cytotoxic effects were observed.

In addition, the cytotoxic effect of several compounds was also tested on single cell level using murine DC. The various compounds (1 μM) were applied alone or followed by administration of the DC activator lipopolysaccharide (100 ng/mL) required to achieve robust T cell stimulatory activity. Neither compound exerted major cytotoxic activity on CD11c$^+$ DC at concentrations about 1,000-fold higher than their $K_i$ values as assessed using membrane impermeable fixable viability dye, which binds to amines of cytoplasmic proteins of dead cells with a porous cell membrane (Figure 11).

## Conclusions

Here, we have demonstrated that α-fluorovinylsulfones and -sulfonates are potent covalent-reversible cathepsin S inhibitors. Both warheads are well suitable for the target enzyme, with the α-fluorovinylsulfonates being more effective. Starting from the K11777 scaffold, we replaced residues in the P2 and P3 positions, resulting in high affinity compounds, some of them being highly selective against off-target cathepsins. In the P3 position, we observed a morpholyl (**3c**) or 4-pyridyl (**3d**) residue to be most suitable with $K_i$ values in the subnanomolar range and moderate selectivity. In the P2 position, we found that cyAla (**4a**, **5a**) increased the selectivity immensely with $K_i$ values in the low nanomolar range for the on-target CatS. Combining the best-performing residues of P2 and P3 to form a morpholyl-cyAla-hPhe-F-vinylsulfonate-Ph motif (**6c**) proved to be most effective with subnanomolar affinity ($K_i$ = 0.09 nM, $K_i$* = 0.01 nM) and exceptional selectivity towards cathepsins B and L (>150,000/125,000-fold). The time-dependent inhibition enables slow-tight binding, thus prolonging target residence times.

Therefore, compound **6c** will be an excellent candidate for further optimizations regarding new small molecule immunomodulators in cancer therapy, where already resistances to existing immunotherapies are known.[26] Cell viability experiments using a non-CatS sensitive cancer cell line and murine derived dendritic cells both did not show cytotoxic effects for all tested inhibitors at relevant concentrations (>1,000-fold $K_i$). The next steps include immunoassays with macrophages or dendritic cells to evaluate the potential of our CatS inhibitors, e.g., for immune cell polarization. This could involve markers like MHC-I and MHC-II expression as well as functional assays for T cell activation.

Moreover, development of inhibitor-nanocarrier constructs is possible with these compounds. By attaching cathepsin S inhibitors to nanocarriers, their efficacy could be further enhanced through specific targeting, e.g., to dendritic cells or other APC.[25] Compound **6b** with a free amino moiety ($K_i$ = 9 nM, SI > 1,000) allows the attachment of various functionalities, such as linkers or nanodelivery systems.

## Experimental Section

### General

All reagents and solvents were purchased from Sigma-Aldrich, Alfa Aesar, Acros, TCI, BLD Pharmatech, Carbolution or Carl Roth in analytical or HPLC grade quality. Chemicals were used without further purification, whereas solvents were distilled and desiccated by standard methods if necessary. $^1$H and $^{13}$C spectra were recorded on a Bruker Fourier 300 device using DMSO-$d_6$ or $CDCl_3$ as solvents. Chemical shifts $\delta$ are given in parts per million (ppm) using residual proton peaks of the solvent as internal standard ($^1$H/$^{13}$C: DMSO 2.50/39.52 ppm; $CHCl_3$ 7.26/77.16 ppm). The compound purity was determined via HPLC-MS at $\lambda$ = 254 nm using an Agilent 1100 series HPLC with an Agilent Poroshell 120 EC-$C_{18}$ column (150×2.10 mm, 4 μm) coupled with an Agilent 1100 series LC/MSD Trap with electron spray ionization (ESI) in positive mode. All compounds tested in enzymatic assays are ≥95% pure by HPLC analysis. The mobile phase consisted of a variable mixture of ACN and $H_2O$ with 0.01% formic acid. For purification we used a Varian PrepStar system (model 218) with a MZ-Aqua Perfect $C_{18}$ column (250×20 mm, 7 μm) by MZ-Analysentechnik. Column chromatography was performed with silica gel (0.040–0.063 mm) and all reactions were monitored by thin-layer chromatography using Macherey-Nagel Alugram Xtra SIL G/UV254 silica gel 60 plates for detection at $\lambda$ = 254 nm. Melting points were determined in open capillaries with a Schorpp Device Technology MPM-H3 instrument. Optical rotation $[\alpha]_D^{22}$ was measured on a Krss P3000 polarimeter (c = 10 mg/mL in MeOH) at 22 °C.

### Syntheses

#### *General procedures*

#### Procedure A (HWE olefination)

The respective phosphonate (1.0 eq) was dissolved in dry THF and cooled to −78 °C. Then, 1 M KHMDS or LHMDS in THF (1.3 eq) was added dropwise and stirred for 30 min, followed by addition of boc-L-homophenylalaninal (**14**, 1.1 eq). The mixture was stirred for 3–5 h at −78 °C and stopped by adding water. The solvent was evaporated under reduced pressure and the residue was extracted with EA (3×), washed with water (2×), sat. aq. $NaHCO_3$ (2×), and brine (2×), then dried over $Na_2SO_4$. Purification by column chromatography.

#### Procedure B (amide couplings)

The carboxylic acid (1.2 eq) was dissolved in DCM or a mixture of DCM/DMF, and cooled to 0 °C. Then, HOBt (1.2 eq), TBTU (1.2 eq), and DIPEA (3.5 eq) were added, and the mixture was stirred for 20 min until all components dissolved. The respective amine (1.0 eq) was added, and the mixture was stirred for an additional 12–24 h, then stopped by adding water. The mixture was extracted with DCM (2×) and the combined organic extracts were washed with water (2×), sat. aq. $NaHCO_3$ (2×), and brine (2×). After drying the crude product over $Na_2SO_4$, it was purified by column chromatography.

#### Procedure C (boc deprotection)

HCl (4 M) in dioxane was added dropwise to the boc-protected amine (1.0 eq) until all components dissolve. The mixture was stirred for 2–12 h and the product was precipitated with diethyl ether and lyophilized afterwards.

#### Procedure D (alkaline hydrolysis)

The ester (1.0 eq) was dissolved in THF. LiOH monohydrate (4.0 eq) was dissolved in water and added to the reaction dropwise. The mixture was stirred for 12–24 h, then the solvent was removed under reduced pressure. The pH of the aqueous phase was adjusted with $KHSO_4$ to 5, giving the products as solids that were further lyophilized.

#### Starting material preparation

#### Ethyl (S)-2-isocyanato-3-phenylpropanoate (7)

Phenylalanine ethyl ester (1.0 eq, 10 mmol, 2.2 g) was dissolved in DCM and an sat. aq. $NaHCO_3$ solution and cooled to 0 °C. Triphosgene (0.33 eq, 3.3 mmol, 0.99 g) was added and the mixture was stirred for 1 h. The mixture was extracted with DCM (2×) and the combined organic extracts were washed with sat. aq. $NaHCO_3$ (2×), and brine (2×), then dried over $Na_2SO_4$ and concentrated under reduced pressure, resulting in the crude product that was used without further purification (1.4 g, 6.4 mmol, 64%). $^1$H NMR (300 MHz, $CDCl_3$) $\delta$[ppm] = 7.35–7.03 (m, 5H), 4.73–4.51 (m, 1H), 4.30–4.07 (m, 2H), 3.16–2.91 (m, 2H), 1.32–1.09 (m, 3H). $^{13}$C NMR (75 MHz, $CDCl_3$) $\delta$[ppm] = 170.7, 135.7, 129.5, 128.7, 127.5, 62.7, 58.7, 40.1, 14.2. $[\alpha]_D^{22} = -9°$.

#### Ethyl (*S*)-2-amino-3-cyclohexylpropanoate (8)

(*S*)-2-Amino-3-cyclohexylpropanoic acid (1.0 eq, 10 mmol, 1.7 g) was dissolved in EtOH and $SOCl_2$ (1.1 eq, 11 mmol, 0.8 mL) was added dropwise. The mixture was stirred under reflux for 12 h and the reaction was stopped with sat. aq. $NaHCO_3$. The solvent was evaporated under reduced pressure and the residue was extracted with EA, giving the crude product that was used without further purification (1.4 g, 7.0 mmol, 68%). $^1$H NMR (300 MHz, $CDCl_3$) $\delta$[ppm] = 4.20–4.01 (m, 2H), 4.00–3.83 (m, 2H, $NH_2$), 3.75 (tt, $J$ = 9.3, 7.0 Hz, 1H), 1.90 (t, $J$ = 7.0 Hz, 2H), 1.65–1.31 (m, 11H), 1.24 (t, $J$ =

8.0 Hz, 3H). $^{13}$C NMR (75 MHz, $CDCl_3$) $\delta$[ppm] = 173.1, 60.5, 54.7, 36.9, 33.4, 33.0, 26.2, 25.5, 13.9. $[\alpha]_D^{22} = -25°$.

### Phosphonate preparation

#### Diethyl ((phenylsulfonyl)methyl)phosphonate (9)

Phenyl methylsulfone (1.0 eq, 15 mmol, 2.2 g) was dissolved in dry THF and cooled to 0 °C. After dropwise addition of 2.5 M *n*-BuLi in hexanes (2.5 eq, 37.5 mmol, 15 mL), the mixture was stirred for 30 min. Then, DECP (1.1 eq, 16.5 mmol, 2.71 mL) was added and the mixture was stirred for 3 h. The reaction was stopped with acetic acid, and the solvent was evaporated under reduced pressure. The residue was extracted with EA (3×) and the combined extracts were washed with water (2×), and brine (2×), then dried over $Na_2SO_4$. The crude product was purified using column chromatography (CH:EA 1:3 – 100% EA), resulting in a yellow oil (3.6 g, 12.3 mmol, 82%). $^1$H NMR (300 MHz, DMSO-$d_6$) $\delta$[ppm] = 8.00–7.90 (m, 2H), 7.79–7.54 (m, 3H), 4.44 (d, $J$ = 17.0 Hz, 2H), 4.06–3.88 (m, 4H), 1.21–1.04 (m, 6H). $^{13}$C NMR (75 MHz, DMSO-$d_6$) $\delta$[ppm] = 140.5, 133.8, 129.0, 127.8, 62.3, 52.3, 50.6, 16.0.

#### Phenyl (diethoxyphosphoryl)methanesulfonate (10)

Phenyl methanesulfonate (1.0 eq, 67 mmol, 11.54 g) was dissolved in dry THF and cooled to −78 °C. Then, 1 M KHMDS (1.3 eq, 88 mmol, 88 mL) was added dropwise and the mixture was stirred for 30 min. Afterwards, DECP (1.1 eq, 74 mmol, 12.2 mL) was added and the mixture was stirred for 3 h and stopped by adding sat. aq. $NH_4Cl$. The solvent was evaporated under reduced pressure and the residue was extracted with EA (3×). The combined extracts were washed with water (2×), and brine (2×), then dried over $Na_2SO_4$. The crude product was purified by column chromatography (CH:EA 1:2 – 100% EA), resulting in a colorless oil (9.0 g, 29 mmol, 43%). $^1$H NMR (300 MHz, DMSO-$d_6$) $\delta$[ppm] = 7.55–7.44 (m, 2H), 7.42–7.31 (m, 3H), 4.63 (d, $J$ = 17.4 Hz, 2H), 4.24–4.05 (m, 4H), 1.25 (t, $J$ = 7.0 Hz, 6H). $^{13}$C NMR (75 MHz, DMSO-$d_6$) $\delta$[ppm] = 148.9, 130.2, 127.5, 122.3, 62.9, 47.7, 45.9, 16.1.

#### Diethyl (fluoro(phenylsulfonyl)methyl)phosphonate (11)

**9** (1.0 eq, 18 mmol, 5.4 g) was dissolved in dry THF and cooled to −78 °C. Then, 1 M LHMDS in THF (1.3 eq, 24 mmol, 24 mL) was added dropwise and the mixture was stirred for 30 min. Afterwards, *Selectfluor* (1.5 eq, 27 mmol, 9.6 g) was dissolved in DMF and added to the mixture. It was stirred for 4 h at 0 °C and stopped by adding sat. aq. $NH_4Cl$. The solvent was evaporated under reduced pressure and the residue was extracted with DCM (3×). The combined extracts were washed with water (2×), sat. aq. $NaHCO_3$ (2×), and brine (2×), then dried over $Na_2SO_4$. The crude product was purified by column chromatography (CH:EA 2:1–1:2), resulting in a colorless solid (2.5 g, 8.0 mmol, 45%). $^1$H NMR (300 MHz, DMSO-$d_6$) $\delta$[ppm] = 8.00–7.92 (m, 2H), 7.88–7.76 (m, 1H), 7.77–7.65 (m, 2H), 6.62 (dd, $J$ = 42.8, 6.8 Hz, 1H), 4.27–4.02 (m, 4H), 1.30–1.16 (m, 6H). $^{13}$C NMR (75 MHz, DMSO-$d_6$) $\delta$[ppm] = 136.2, 135.2, 129.5, 129.3, 64.3, 64.1, 16.1. MP = 67–69 °C.

#### Phenyl (diethoxyphosphoryl)fluoromethanesulfonate (12)

**10** (1.0 eq, 28 mmol, 8.9 g) was dissolved in dry THF and cooled to −78 °C. Then, 1 M LHMDS in THF (1.3 eq, 37 mmol, 37 mL) was added dropwise and the mixture was stirred for 30 min. Afterwards, *Selectfluor* (1.5 eq, 42.5 mmol, 15.0 g) was dissolved in DMF and added to the mixture. It was allowed to warm to 0 °C, stirred for 4 h, and stopped by adding sat. aq. $NH_4Cl$. The solvent was evaporated under reduced pressure and the residue was extracted with DCM (3×). The combined extracts were washed with water (2×), sat. aq. $NaHCO_3$ (2×), and brine (2×), then dried over $Na_2SO_4$. The crude product was purified by column chromatography (CH:EA 2:1–1:2), resulting in a colorless oil (4.4 g, 13.3 mmol, 46%). $^1$H NMR (300 MHz, $CDCl_3$) $\delta$[ppm] = 7.40–7.19 (m, 2H), 7.22–7.02 (m, 3H), 5.66 (dd, $J$ = 45.2, 7.2 Hz, 1H), 4.37–4.18 (m, 1H), 4.18–4.02 (m, 4H), 1.41–1.14 (m, 6H). $^{13}$C NMR (75 MHz, $CDCl_3$) $\delta$[ppm] = 129.6, 127.8, 124.8, 122.0, 119.9, 64.5, 15.9.

### Aldehyde preparation

#### *tert*-Butyl (*S*)-(1-(methoxy(methyl)amino)-1-oxo-4-phenylbutan-2-yl) carbamate (13)

Boc-L-homophenylalanine (1.2 eq, 18 mmol, 5.0 g) was dissolved in DCM and cooled to 0 °C. Then, HOBt (1.2 eq, 18 mmol, 2.4 g), TBTU (1.2 eq, 18 mmol, 5.8 g), and DIPEA (3.5 eq, 52.5 mmol, 9.2 mL) were added and the mixture was stirred for 20 min until all components were dissolved. *N,O*-Dimethyl hydroxylamine (1.0 eq, 15 mmol, 1.5 g) was added and the mixture was stirred for an additional 12–24 h, then stopped by adding water. The mixture was extracted with DCM (2×) and the combined organic extracts were washed with water (2×), sat. aq. $NaHCO_3$ (2×), and brine (2×). After drying the crude product over $Na_2SO_4$, it was purified by column chromatography (CH:EA 2:1–1:4), giving the product as a colorless oil (4.8 g, 15 mmol, 100%). $^1$H NMR (300 MHz, DMSO-$d_6$) $\delta$[ppm] = 6.77–6.65 (m, 2H), 6.66–6.51 (m, 3H), 3.82–3.65 (m, 1H), 2.99 (s, 3H), 2.76 (s, 3H), 2.22–2.03 (m, 1H), 2.01–1.87 (m, 2H), 1.23 (q, $J$ = 7.0, 6.4 Hz, 2H), 0.91–0.78 (m, 9H). $^{13}$C NMR (75 MHz, DMSO-$d_6$) $\delta$[ppm] = 155.6, 141.1, 128.4, 128.2, 125.8, 77.9, 60.9, 50.09, 40.4, 40.1, 39.8, 39.5, 39.2, 39.0, 38.7, 32.3, 31.6, 28.2, 26.3. $[\alpha]_D^{22} = -40°$.

#### *tert*-Butyl (*S*)-(1-oxo-4-phenylbutan-2-yl)carbamate (14)

**13** (1.0 eq, 15 mmol, 5.2 g) was dissolved in dry diethyl ether and cooled to 0 °C. $LiAlH_4$ (1.3 eq, 19.5 mmol, 0.74 g) was added in portions and the mixture was stirred for 2 h. Afterwards, the reaction was stopped with 0.33 M $KHSO_4$ and the mixture was extracted with diethyl ether (2×). The combined extracts were washed with water (2×), 1 M HCl (2×), sat. aq. $NaHCO_3$ (2×), and brine (2×). The product was dried over $Na_2SO_4$, resulting in a colorless oil that solidified upon standing (3.9 g, 14.7 mmol, 99%). $^1$H NMR (300 MHz, $CDCl_3$) $\delta$[ppm] = 9.55 (s, 1H), 7.46–7.00 (m, 5H), 5.07 (s, 1H), 4.37–4.09 (m, 1H), 2.71 (t, $J$ = 7.5 Hz, 2H), 2.37–2.01 (m, 2H), 1.56–1.28 (m, 9H). $^{13}$C NMR (75 MHz, $CDCl_3$) $\delta$[ppm] = 199.7, 128.8, 128.6, 126.5, 77.6, 77.2, 76.7, 66.0, 31.6, 31.1, 28.4, 15.4. $[\alpha]_D^{22} = -28°$.

### Warhead preparation

#### *tert*-Butyl (*S,E*)-(1-fluoro-5-phenyl-1-(phenylsulfonyl)pent-1-en-3-yl)carbamate (15)

**15** was prepared according to procedure A using 1 M LHMDS (2.6 mmol, 2.6 mL), phosphonate **11** (2.0 mmol, 0.60 g), and aldehyde 14 (2.2 mmol, 0.58 g). Purification by column chromatography (CH:EA 6:1–4:1) resulted in a colorless oil (0.50 g, 1.2 mmol, 59%). $^1$H NMR (300 MHz, $CDCl_3$) $\delta$[ppm] = 8.10 (s, 2H), 7.77–7.51 (m, 3H), 7.40–7.19 (m, 5H), 5.85 (dd, $J_{H\text{-}F}$ = 21.3 Hz, $J_{H\text{-}H}$ = 10.1 Hz, 1H), 5.38–5.22 (m, 1H), 4.81–4.68 (m, 1H), 2.80 (ddd, $J$ = 16.9, 10.2, 6.0 Hz, 2H), 2.13–1.80 (m, 2H), 1.47 (s, 9H). $^{13}$C NMR (75 MHz, $CDCl_3$)

$\delta$[ppm] = 149.8 (d, $J_{C\text{-}F}$ = 299 Hz), 140.8, 137.6, 134.5, 129.4, 128.9, 128.6, 128.4, 126.2, 121.0 (d, $J_{C\text{-}F}$ = 4.2 Hz), 77.0, 46.1 (d, $J_{C\text{-}F}$ = 2.2 Hz), 32.0, 31.0, 28.3. $[\alpha]_D^{22} = -10°$.

### Phenyl (*S,E*)-3-((*tert*-butoxycarbonyl)amino)-1-fluoro-5-phenyl-pent-1-ene-1-sulfonate (16)

**16** was prepared according to procedure A using phosphonate **12** (4.0 mmol, 1.3 g). Purification by column chromatography (CH:EA 5:1–3:1) resulted in a colorless oil (0.80 g, 1.8 mmol, 46%). $^1$H NMR (300 MHz, $CDCl_3$) $\delta$[ppm] = 7.46–7.32 (m, 2H), 7.32–7.15 (m, 6H), 7.10 (d, $J$ = 7.0 Hz, 2H), 5.91 (dd, $J_{H\text{-}F}$ = 31.3 Hz, $J_{H\text{-}H}$ = 8.6 Hz, 1H), 4.68–4.27 (m, 2H), 2.66–2.43 (m, 2H), 1.97–1.66 (m, 2H), 1.43 (s, 9H). $^{13}$C NMR (75 MHz, $CDCl_3$) $\delta$[ppm] = 154.8, 150.8, 148.9 (d, $J_{C\text{-}F}$ = 296 Hz), 140.2, 130.2, 128.8, 128.4, 128.0, 126.5, 122.4 (d, $J_{C\text{-}F}$ = 4.1 Hz), 122.3, 80.4, 46.3 (d, $J_{C\text{-}F}$ = 2.1 Hz), 35.9, 31.9, 28.4. $[\alpha]_D^{22} = -15°$.

### (S,E)-1-Fluoro-5-phenyl-1-(phenylsulfonyl)pent-1-en-3-aminium chloride (17)

**17** was prepared according to procedure C using **15** (1.2 mmol, 0.50 g), resulting in a colorless solid (0.39 g, 1.1 mmol, 95%). $^1$H NMR (300 MHz, DMSO-$d_6$) $\delta$[ppm] = 8.71 (s, 3H), 8.02 (dd, $J$ = 7.3, 1.7 Hz, 2H), 7.97–7.82 (m, 1H), 7.76 (dd, $J$ = 8.4, 7.0 Hz, 2H), 7.28–7.10 (m, 3H), 7.11–7.02 (m, 2H), 6.55 (dd, $J_{H\text{-}F}$ = 32.6 Hz, $J_{H\text{-}H}$ = 9.8 Hz, 1H), 4.07–3.94 (m, 1H), 2.57–2.39 (m, 2H), 2.26–1.95 (m, 2H). $^{13}$C NMR (75 MHz, DMSO-$d_6$) $\delta$[ppm] = 154.6 (d, $J_{C\text{-}F}$ = 298 Hz), 140.3, 136.4, 136.1, 130.7, 130.2, 129.0, 128.9, 128.6, 126.7, 115.0 (d, $J_{C\text{-}F}$ = 3.5 Hz), 45.5 (d, $J_{C\text{-}F}$ = 2.6 Hz), 33.9 (d, $J_{C\text{-}F}$ = 1.3 Hz), 31.0. $[\alpha]_D^{22} = -15°$. MP = 130–132 °C.

### Phenyl (S,E)-3-amino-1-fluoro-5-phenylpent-1-ene-1-sulfonate hydrochloride (18)

**18** was prepared according to procedure C using **16** (1.7 mmol, 0.73 g), resulting in a colorless solid (0.55 g, 1.5 mmol, 88%). $^1$H NMR (300 MHz, DMSO-$d_6$) $\delta$[ppm] = 8.77 (s, 3H), 7.59–7.50 (m, 2H), 7.49–7.39 (m, 3H), 7.36 (t, $J$ = 7.2 Hz, 2H), 7.28–7.21 (m, 1H), 7.21–7.11 (m, 2H), 6.45 (dd, $J_{H\text{-}F}$ = 32 Hz, $J_{H\text{-}H}$ = 9.7 Hz, 1H), 4.15 (td, $J$ = 9.2, 5.3 Hz, 1H), 2.52–2.36 (m, 2H), 2.22–2.03 (m, 1H), 2.02–1.85 (m, 1H). $^{13}$C NMR (75 MHz, DMSO-$d_6$) $\delta$[ppm] = 149.7 (d, $J_{C\text{-}F}$ = 300 Hz), 149.0, 140.4, 130.9, 129.3, 129.2, 128.9, 126.4, 122.3, 118.6 (d, $J_{C\text{-}F}$ = 3.2 Hz), 45.5 (d, $J_{C\text{-}F}$ = 2.2 Hz), 40.5, 33.6, 30.5. $[\alpha]_D^{22} = -13°$. MP = 141–143 °C.

## Dipeptide preparation

### Ethyl (4-methylpiperazine-1-carbonyl)-l-phenylalaninate (19)

Compound **7** (1.0 eq, 8.5 mmol, 1.9 g) was dissolved in THF and cooled to 0 °C. Then, *N*-methyl piperazine (1.1 eq, 9.3 mmol, 1.0 mL) was added dropwise. After 12 h, THF was removed under reduced pressure and the residue was extracted with EA (3×). The combined organic extracts were washed with water (2×), sat. aq. $NaHCO_3$ (2×), and brine (2×). The organic layer was dried with $Na_2SO_4$ and evaporated. Purification by column chromatography (DCM:MeOH 19:1) resulted in a colorless solid (2.4 g, 7.4 mmol, 87%). $^1$H NMR (300 MHz, DMSO-$d_6$) $\delta$[ppm] = 7.35–7.09 (m, 5H), 6.79 (d, $J$ = 7.9 Hz, 1H, NH), 4.23 (ddd, $J$ = 8.9, 7.8, 6.5 Hz, 1H), 4.01 (qd, $J$ = 7.1, 1.7 Hz, 2H), 3.24 (q, $J$ = 4.5 Hz, 4H), 3.04–2.83 (m, 2H), 2.20–2.15 (m, 4H), 2.13 (s, 3H), 1.09 (t, $J$ = 7.1 Hz, 3H). $^{13}$C NMR (75 MHz, DMSO-$d_6$) $\delta$[ppm] = 173.0, 157.2, 138.0, 129.3, 128.3, 126.5, 60.3, 55.7, 54.4, 45.8, 43.5, 36.8, 14.1. $[\alpha]_D^{22} = -18°$. MP = 97–99 °C.

### (4-Methylpiperazine-1-carbonyl)-L-phenylalanine (20)

**20** was prepared according to procedure D using **19** (7.4 mmol, 2.4 g), resulting in a colorless solid (1.8 g, 6.3 mmol, 85%). $^1$H NMR (300 MHz, DMSO-$d_6$) $\delta$[ppm] = 7.33–7.05 (m, 5H), 6.68 (d, $J$ = 7.9 Hz, 1H), 4.28 –4.09 (m, 1H), 3.50–3.16 (m, 4H), 2.98 (m, 2H), 2.46–2.30 (m, 4H), 2.25 (s, 3H). $^{13}$C NMR (75 MHz, DMSO-$d_6$) $\delta$[ppm] = 174.6, 157.1, 139.0, 129.4, 128.0, 126.1, 56.0, 53.1, 44.8, 42.7, 39.5, 36.9. $[\alpha]_D^{22} = -17°$. MP = 121–123 °C.

### *tert*-Butyl (*S*)-4-((1-ethoxy-1-oxo-3-phenylpropan-2-yl)carbamoyl) piperazine-1-carboxylate (21)

1-Boc piperazine (1.1 eq, 1.3 mmol, 0.24 g) was dissolved in THF. Compound **7** (1.0 eq, 1.2 mmol, 0.27 g) was added dropwise, and the mixture was stirred for 18 h at room temperature. Then, the solvent was evaporated, and the residue was extracted with EA (3×). The combined organic extracts were washed with water (2×), sat. aq. $NaHCO_3$ (2×), and brine. The crude product was dried with $Na_2SO_4$, and the solvent was evaporated under reduced pressure. Purification by column chromatography (DCM:MeOH 49:1) gave the product as a colorless oil (0.41 g, 1.0 mmol, 84%). $^1$H NMR (300 MHz, $CDCl_3$) $\delta$[ppm] = 7.33–7.18 (m, 3H), 7.11 (dd, $J$ = 7.7, 1.8 Hz, 2H), 4.89 (d, $J$ = 7.5 Hz, 1H, NH), 4.76 (q, $J$ = 6.1 Hz, 1H), 4.17 (q, $J$ = 7.1 Hz, 2H), 3.48–3.23 (m, 8H), 3.09 (dd, $J$ = 13.1, 5.8 Hz), 1.85 (s, 1H), 1.46 (s, 9H), 1.24 (td, $J$ = 7.1, 1.0 Hz, 3H). $^{13}$C NMR (75 MHz, $CDCl_3$) $\delta$[ppm] = 172.7, 156.6, 154.7, 136.3, 129.5, 128.6, 127.2, 80.3, 61.6, 54.5, 53.6, 43.6, 38.5, 28.5, 14.3. $[\alpha]_D^{22} = -24°$.

### (4-(*tert*-Butoxycarbonyl)piperazine-1-carbonyl)-l-phenylalanine (22)

**22** was prepared according to procedure D using **21** (0.94 mmol, 0.38 g), resulting in a colorless solid (0.27 g, 0.71 mmol, 76%). $^1$H NMR (300 MHz, $CDCl_3$) $\delta$[ppm] = 8.79 (s, 1H, OH), 7.33–7.22 (m, 3H), 7.20–7.14 (m, 2H), 5.07 (d, $J$ = 7.1 Hz, 1H, NH), 4.65 (q, $J$ = 6.4 Hz, 1H), 3.42–3.21 (m, 8H), 3.21–3.04 (m, 2H), 1.45 (s, 9H). $^{13}$C NMR (75 MHz, $CDCl_3$) $\delta$[ppm] = 174.7, 157.5, 154.8, 136.4, 129.5, 128.8, 127.3, 80.6, 55.0, 43.7, 37.4, 28.5. $[\alpha]_D^{22} = -23°$. MP = 82–84 °C.

### Ethyl (morpholine-4-carbonyl)-L-phenylalaninate (23)

Compound **7** (1.0 eq, 4.5 mmol, 1.0 g) was dissolved in THF and cooled to 0 °C. Then, DIPEA (2.5 eq, 11 mmol, 2.0 mL) and morpholine (1.4 eq, 6.4 mmol, 0.55 mL) were added dropwise. After 12 h, THF was removed under reduced pressure and the residue was extracted with EA (3×). The combined organic extracts were washed with water (2×), sat. aq. $NaHCO_3$ (2×), and brine (2×). The organic layer was dried with $Na_2SO_4$ and evaporated, giving a colorless oil (1.3 g, 4.5 mmol, 100%). $^1$H NMR (300 MHz, $CDCl_3$) $\delta$[ppm] = 7.38–7.16 (m, 5H), 7.12 (d, $J$ = 11.7 Hz, 1H, NH), 4.69 (dt, $J$ = 11.7, 7.0 Hz, 1H), 4.27–3.98 (m, 2H), 3.64 (td, $J$ = 7.1, 1.3 Hz, 4H), 3.38 (dt, $J$ = 10.6, 7.1 Hz, 4H), 2.97 (ddt, $J$ = 7.0, 2.6, 0.9 Hz, 2H), 1.22 (t, $J$ = 8.0 Hz, 3H). $^{13}$C NMR (75 MHz, $CDCl_3$) $\delta$[ppm] = 172.1, 157.3, 136.8, 129.2, 128.6, 127.2, 66.0, 61.7, 55.2, 46.7, 37.6, 14.1. $[\alpha]_D^{22} = -19°$.

### (Morpholine-4-carbonyl)-L-phenylalanine (24)

**24** was prepared according to procedure D using **23** (4.5 mmol, 1.3 g), resulting in a colorless oil (0.71 g, 2.7 mmol, 59%). $^1$H NMR

(300 MHz, $CDCl_3$) $\delta$[ppm] = 7.77 (d, $J$ = 11.9 Hz, 1H), 7.31–7.11 (m, 5H), 4.48 (dt, $J$ = 11.9, 7.0 Hz, 1H), 3.64 (td, $J$ = 7.1, 1.7 Hz, 4H), 3.30 (dt, $J$ = 8.8, 7.1 Hz, 4H), 3.03 (dq, $J$ = 7.0, 1.0 Hz, 2H). $^{13}$C NMR (75 MHz, $CDCl_3$) $\delta$[ppm] = 174.8, 157.6, 137.0, 130.1, 128.7, 126.9, 66.0, 56.2, 46.5, 37.5. $[\alpha]_D^{22} = -12°$.

### (S)-Ethyl-2-(isonicotinamido)-3-phenylpropanoate (25)

**25** was prepared according to procedure B using L-phenylalanine ethyl ester hydrochloride (14 mmol, 3.0 g) and isonicotinic acid (15 mmol, 1.9 g). Purification by column chromatography (CH:EA 1:4) gave a colorless oil (3.3 g, 12 mmol, 84%). $^1$H NMR (300 MHz, DMSO-$d_6$) $\delta$[ppm] = 9.18 (d, $J$ = 7.9 Hz, 1H, NH), 8.76–8.68 (m, 2H), 7.72–7.64 (m, 2H), 7.33–7.15 (m, 5H), 4.69 (ddd, $J$ = 10.1, 7.8, 5.2 Hz, 1H), 3.65 (s, 3H), 3.20 (dd, $J$ = 13.7, 5.3 Hz, 1H), 3.08 (dd, $J$ = 13.7, 10.2 Hz, 1H). $^{13}$C NMR (75 MHz, DMSO-$d_6$) $\delta$[ppm] = 171.8, 164.9, 150.3, 140.5, 137.5, 129.1, 128.3, 126.6, 121.3, 54.3, 52.1, 36.2. $[\alpha]_D^{22} = -37°$.

### (S)-2-(Isonicotinamido)-3-phenylpropanoic acid (26)

**26** was prepared according to procedure D using **25** (7.8 mmol, 2.2 g), resulting in a colorless solid (1.4 g, 5.0 mmol, 65%). $^1$H NMR (300 MHz, DMSO-$d_6$) $\delta$[ppm] = 12.87 (s, 1H, OH), 9.04 (d, $J$ = 8.2 Hz, 1H, NH), 8.76–8.66 (m, 2H), 7.74–7.62 (m, 2H), 7.36–7.22 (m, 4H), 7.22–7.13 (m, 1H), 4.64 (ddd, $J$ = 10.7, 8.1, 4.4 Hz, 1H), 3.22 (dd, $J$ = 13.8, 4.5 Hz, 1H), 3.05 (dd, $J$ = 13.8, 10.7 Hz, 1H). $^{13}$C NMR (75 MHz, DMSO-$d_6$) $\delta$[ppm] = 172.8, 164.8, 150.3, 140.8, 138.0, 129.1, 128.3, 126.5, 121.3, 54.3, 36.2. $[\alpha]_D^{22} = -35°$. MP = 166–168 °C.

### Ethyl (thiophene-3-carbonyl)-L-phenylalaninate (27)

**27** was prepared according to procedure B using L-phenylalanine ethyl ester hydrochloride (20 mmol, 4.5 g) and thiophene-3-carboxylic acid (20 mmol, 1.9 g), resulting in a colorless oil (5.5 g, 19 mmol, 95%). $^1$H NMR (300 MHz, $CDCl_3$) $\delta$[ppm] = 8.06 (d, $J$ = 11.9 Hz, 1H, NH), 7.98 (dd, $J$ = 2.7, 1.6 Hz, 1H), 7.73–7.49 (m, 2H), 7.34–7.07 (m, 5H), 4.85 (dt, $J$ = 11.9, 7.0 Hz, 1H), 4.31–3.95 (m, 2H), 3.16–2.89 (m, 2H), 1.34–1.11 (m, 3H). $^{13}$C NMR (75 MHz, $CDCl_3$) $\delta$[ppm] = 171.8, 162.9, 136.8, 134.4, 130.2, 129.9, 129.2, 128.6, 127.2, 125.9, 61.6, 53.9, 37.7, 14.1. $[\alpha]_D^{22} = -25°$.

### (Thiophene-3-carbonyl)-L-phenylalanine (28)

**28** was prepared according to procedure D using **27** (15 mmol, 4.4 g), resulting in a colorless solid (4.0 g, 15 mmol, 100%). $^1$H NMR (300 MHz, $CDCl_3$) $\delta$[ppm] = 9.60 (s, 1H, OH), 8.22 (d, $J$ = 12.1 Hz, 1H, NH), 7.95 (dd, $J$ = 2.8, 1.6 Hz, 1H), 7.76 (dd, $J$ = 7.5, 1.5 Hz, 1H), 7.60 (dd, $J$ = 7.4, 2.8 Hz, 1H), 7.38–7.16 (m, 5H), 4.66 (dt, $J$ = 12.1, 7.0 Hz, 1H), 3.35–3.04 (m, 2H). $^{13}$C NMR (75 MHz, $CDCl_3$) $\delta$[ppm] = 173.8, 163.0, 137.4, 134.6, 130.5, 130.1, 130.0, 128.7, 127.0, 125.4, 54.9, 37.5. $[\alpha]_D^{22} = -20°$. MP = 95–97 °C.

### Ethyl benzoyl-L-phenylalaninate (29)

**29** was prepared according to procedure B using L-phenylalanine ethyl ester hydrochloride (22 mmol, 5.0 g) and benzoic acid (26 mmol, 3.2 g), resulting in a colorless solid (5.2 g, 18 mmol, 80%). $^1$H NMR (300 MHz, $CDCl_3$) $\delta$[ppm] = 8.04 (d, $J$ = 11.9 Hz, 1H, NH), 7.80–7.70 (m, 2H), 7.65–7.49 (m, 1H), 7.41–7.33 (m, 2H), 7.31–7.14 (m, 5H), 4.88 (dt, $J$ = 11.9, 7.0 Hz, 1H), 4.32–3.93 (m, 2H), 3.17–2.90 (m, 2H), 1.26 (t, $J$ = 8.0 Hz, 3H). $^{13}$C NMR (75 MHz, $CDCl_3$) $\delta$[ppm] = 171.8, 167.1, 136.8, 133.8, 131.8, 129.3, 128.9, 128.6, 127.4, 127.2, 61.5, 54.2, 37.80, 14.3. $[\alpha]_D^{22} = -28°$. MP = 115–117 °C.

### Benzoyl-L-phenylalanine (30)

**30** was prepared according to procedure D using **29** (6.4 mmol, 1.9 g), resulting in a colorless solid (1.6 g, 5.8 mmol, 91%). $^1$H NMR (300 MHz, $CDCl_3$) $\delta$[ppm] = 9.55 (s, 1H, OH), 8.29 (d, $J$ = 11.9 Hz, 1H, NH), 7.83–7.60 (m, 3H), 7.51–7.42 (m, 1H), 7.38–7.35 (m, 3H), 7.34–7.15 (m, 7H), 4.67 (dt, $J$ = 12.1, 7.0 Hz, 1H), 3.31–3.07 (m, 3H). $^{13}$C NMR (75 MHz, $CDCl_3$) $\delta$[ppm] = 174.8, 167.0, 137.4, 134.2, 131.7, 130.1, 128.7, 128.7, 127.4, 126.9, 54.8, 37.5. $[\alpha]_D^{22} = -20°$. MP = 148–150 °C.

### Ethyl (S)-3-cyclohexyl-2-(isonicotinamido)propanoate (31)

**31** was prepared according to procedure B using **8** (6.5 mmol, 1.3 g) and isonicotinic acid (7.8 mmol, 0.96 g). Purification by column chromatography (CH:EA 1:1 – 100% EA) resulted in a colorless oil (1.8 g, 5.9 mmol, 93%). $^1$H NMR (300 MHz, $CDCl_3$) $\delta$[ppm] = 8.71–8.53 (m, 2H), 7.65–7.46 (m, 2H), 7.05 (d, $J$ = 8.2 Hz, 1H, NH), 4.77 (ddd, $J$ = 9.0, 8.1, 5.4 Hz, 1H), 4.24–4.08 (m, 2H), 1.96 (s, 2H), 1.82–1.49 (m, 10H), 1.46–1.27 (m, 1H), 1.27–1.11 (m, 3H). $^{13}$C NMR (75 MHz, $CDCl_3$) $\delta$[ppm] = 174.2, 165.3, 150.5, 141.1, 121.1, 61.4, 51.8, 34.4, 33.5, 32.7, 26.4, 26.2, 26.1, 14.2. $[\alpha]_D^{22} = -29°$.

### (S)-3-Cyclohexyl-2-(isonicotinamido)propanoic acid (32)

**32** was prepared according to procedure D using **31** (5.9 mmol, 1.8 g), resulting in a colorless solid (0.80 g, 2.9 mmol, 49%). $^1$H NMR (300 MHz, DMSO-$d_6$) $\delta$[ppm] = 8.89 (d, $J$ = 7.9 Hz, 1H, *NH*), 8.78–8.57 (m, 2H), 7.97–7.61 (m, 2H), 4.47 (ddd, $J$ = 10.4, 7.8, 4.7 Hz, 1H), 1.82–1.49 (m, 6H), 1.51–1.25 (m, 1H), 1.25–0.98 (m, 3H), 1.00–0.77 (m, 3H). $^{13}$C NMR (75 MHz, DMSO-$d_6$) $\delta$[ppm] = 173.9, 165.0, 150.3, 140.9, 121.4, 50.3, 37.9, 33.8, 33.2, 31.5, 26.0, 25.7, 25.6. $[\alpha]_D^{22} = -35°$. MP = 115–117 °C.

### Ethyl isonicotinoyl-L-leucinate (33)

**33** was prepared according to procedure B using L-leucin ethyl ester hydrochloride (6.0 mmol, 1.2 g) and isonicotinic acid (7.2 mmol, 0.9 g), resulting in a yellow oil (1.6 g, 6.0 mmol, 100%). $^1$H NMR (300 MHz, DMSO-$d_6$) $\delta$[ppm] = 8.84 (d, $J$ = 7.7 Hz, 1H), 8.65–8.49 (m, 2H), 7.69–7.51 (m, 2H), 4.45–4.17 (m, 1H), 3.93 (q, $J$ = 7.2 Hz, 2H), 1.69–1.37 (m, 2H), 1.21 (dt, $J$ = 11.8, 6.8 Hz, 1H), 1.00 (t, $J$ = 7.1 Hz, 3H), 0.81–0.56 (m, 6H). $^{13}$C NMR (75 MHz, DMSO-$d_6$) $\delta$[ppm] = 172.6, 165.6, 150.7, 141.2, 121.8, 61.0, 51.6, 39.6, 24.9, 23.2, 21.6, 14.5. $[\alpha]_D^{22} = -28°$.

### Isonicotinoyl-L-leucine (34)

**34** was prepared according to procedure D using **33** (6.0 mmol, 1.6 g), resulting in a yellow solid (1.3 g, 5.4 mmol, 90%). $^1$H NMR (300 MHz, DMSO-$d_6$) $\delta$[ppm] = 9.43 (d, $J$ = 7.7 Hz, 1H, *NH*), 9.08–8.77 (m, 2H), 8.32–8.10 (m, 2H), 4.43 (ddd, $J$ = 11.1, 7.7, 4.2 Hz, 1H), 1.99–1.72 (m, 1H), 1.72–1.43 (m, 2H), 1.00–0.66 (m, 6H). $^{13}$C NMR (75 MHz, DMSO-$d_6$) $\delta$[ppm] = 173.8, 164.1, 146.2, 145.6, 124.2, 39.9, 51.8, 25.0, 23.4, 21.6. $[\alpha]_D^{22} = -14°$. MP = 122–124 °C.

### Ethyl (S)-2-(isonicotinamido)-4-phenylbutanoate (35)

**35** was prepared according to procedure B using L-homophenylalanine ethyl ester hydrochloride (6.0 mmol, 1.5 g) and isonicotinic acid (7.2 mmol, 0.89 g), resulting in a yellow solid (1.2 g, 3.8 mmol, 67%). $^1$H NMR (300 MHz, DMSO-$d_6$) $\delta$[ppm] = 8.99–8.81 (m, 1H, *NH*), 8.66–8.47 (m, 2H), 7.62 (dt, $J$ = 4.5, 1.8 Hz, 2H), 7.17–6.89 (m, 5H), 4.20 (qd, $J$ = 7.4, 1.7 Hz, 1H), 4.00–3.85 (m, 2H), 2.61–2.50 (m, 2H),

1.98–1.84 (m, 2H), 0.99 (td, $J$=7.1, 1.7 Hz, 3H). $^{13}$C NMR (75 MHz, DMSO-$d_6$) $\delta$[ppm]=172.2, 165.8, 150.7, 141.3, 141.2, 128.9, 128.8, 126.5, 121.9, 61.1, 52.8, 32.7, 32.1, 14.5. $[\alpha]_D^{22}=-30°$. MP=101–103 °C.

### (S)-2-(Isonicotinamido)-4-phenylbutanoic acid (36)

**36** was prepared according to procedure D using **35** (3.8 mmol, 1.2 g), resulting in a yellow solid (0.6 g, 2.1 mmol, 56%). $^1$H NMR (300 MHz, DMSO-$d_6$) $\delta$[ppm]=12.72 (s, 1H, *OH*), 9.01 (d, $J$=7.7 Hz, 1H, *NH*), 8.75 (q, $J$=2.2 Hz, 2H), 7.81 (q, $J$=2.3 Hz, 2H), 7.46–7.03 (m, 5H), 4.34 (q, $J$=7.6, 7.1 Hz, 1H), 2.92–2.51 (m, 2H), 2.23–1.94 (m, 2H). $^{13}$C NMR (75 MHz, DMSO-$d_6$) $\delta$[ppm]=173.8, 165.7, 150.7, 141.4, 128.9, 128.8, 126.4, 121.9, 52.7, 32.7, 32.2. $[\alpha]_D^{22}=-31°$. MP=133–135 °C.

### Ethyl isonicotinoyl-L-tryptophanate (37)

**37** was prepared according to procedure B using L-tryptophane ethyl ester hydrochloride (6.0 mmol, 1.6 g) and isonicotinic acid (7.2 mmol, 0.89 g), resulting in a yellow oil (2.0 g, 6.0 mmol, 100%). $^1$H NMR (300 MHz, $CDCl_3$) $\delta$[ppm]=8.70–8.60 (m, 2H), 8.54 (s, 1H, *NH*), 7.55–7.49 (m, 1H), 7.49–7.42 (m, 2H), 7.35 (dt, $J$=8.2, 1.0 Hz, 1H), 7.22–7.02 (m, 2H), 7.00 (d, $J$=2.4 Hz, 1H), 6.82 (d, $J$=7.7 Hz, 1H), 5.10 (dt, $J$=7.7, 5.3 Hz, 1H), 4.19 (qd, $J$=7.2, 4.2 Hz, 2H), 3.54–3.35 (m, 2H), 1.26 (t, $J$=7.1 Hz, 3H). $^{13}$C NMR (75 MHz, $CDCl_3$) $\delta$[ppm]=171.7, 165.1, 150.5, 141.2, 136.3, 127.8, 123.0, 122.5, 121.1, 119.9, 118.6, 111.6, 109.8, 61.9, 53.9, 27.6, 14.2. $[\alpha]_D^{22}=-14°$.

### Isonicotinoyl-L-tryptophan (38)

**38** was prepared according to procedure D using **37** (6.0 mmol, 2.0 g), resulting in an orange solid (0.81 g, 2.6 mmol, 44%). $^1$H NMR (300 MHz, DMSO-$d_6$) $\delta$[ppm]=10.93 (d, $J$=2.4 Hz, 1H, *OH*), 9.00 (d, $J$=7.9 Hz, 1H, *NH*), 8.82–8.54 (m, 2H), 7.78–7.69 (m, 2H), 7.59 (d, $J$=7.8 Hz, 1H), 7.32 (d, $J$=8.0 Hz, 1H), 7.22 (d, $J$=2.3 Hz, 1H), 7.10–6.91 (m, 2H), 4.66 (ddd, $J$=9.5, 7.8, 4.5 Hz, 1H), 3.45–3.12 (m, 2H). $^{13}$C NMR (75 MHz, DMSO-$d_6$) $\delta$[ppm]=173.3, 164.8, 150.2, 141.0, 136.1, 127.2, 123.7, 121.4, 120.9, 118.3, 118.2, 111.5, 110.4, 54.2, 26.7. $[\alpha]_D^{22}=-10°$. MP=150–152 °C.

### Ethyl (*S*)-2-(4-((*tert*-butoxycarbonyl)amino)benzamido)-3-cyclohexylpropanoate (39)

**39** was prepared according to procedure B using *N*-boc-4-amino benzoic acid (7.5 mmol, 1.5 g), resulting in a colorless solid (3.1 g, 7.5 mmol, 100%). $^1$H NMR (300 MHz, $CDCl_3$) $\delta$[ppm]=7.97–7.85 (m, 1H), 7.62–7.38 (m, 4H), 6.38 (d, $J$=8.2 Hz, 1H), 4.61 (td, $J$=8.5, 5.6 Hz, 1H), 3.99 (qd, $J$=7.1, 1.9 Hz, 2H), 2.58 (s, 1H), 1.66–1.52 (m, 2H), 1.33–0.89 (m, 18H), 0.92–0.49 (m, 3H). $^{13}$C NMR (75 MHz, $CDCl_3$) $\delta$[ppm]=173.5, 166.7, 152.6, 142.0, 132.3, 128.3, 128.1, 117.8, 81.0, 61.4, 50.7, 34.4, 33.5, 32.8, 28.4, 28.3, 26.4, 26.2, 26.1, 14.2. $[\alpha]_D^{22}=-12°$. MP=87–89 °C.

### (S)-2-(4-((tert-Butoxycarbonyl)amino)benzamido)-3-cyclohexylpropanoic acid (40)

**40** was prepared according to procedure D using **39** (7.5 mmol, 3.1 g), resulting in a colorless solid (2.7 g, 6.9 mmol, 92%). $^1$H NMR (300 MHz, DMSO-$d_6$) $\delta$[ppm]=9.47 (d, $J$=32.7 Hz, 1H), 8.18 (d, $J$=7.9 Hz, 1H), 7.78–7.49 (m, 2H), 7.46–7.19 (m, 2H), 4.45–4.11 (m, 1H), 3.54–3.07 (m, 2H), 2.37–2.08 (m, 1H), 1.64–1.29 (m, 10H), 1.40–1.21 (m, 9 H). $^{13}$C NMR (75 MHz, DMSO) $\delta$[ppm]=174.9, 167.5, 153.0, 144.2, 130.8, 124.5, 117.7, 117.5, 80.1, 50.6, 34.3, 33.7, 31.9, 28.5, 28.5, 26.5, 25.6. $[\alpha]_D^{22}=-11°$. MP=104–106 °C.

### (4-Morpholine-1-carbonyl)-L-cyclohexylalanine methylester (41)

L-Cyclohexylalanine methylester hydrochloride (1.0 eq, 2.48 mmol, 0.55 g) was dissolved in DCM and a sat. aq. $NaHCO_3$ (40 mL) solution and cooled to 0 °C. Triphosgene (0.33 eq, 0.83 mmol, 0.25 g) was added and the mixture was stirred for 30 min. The mixture was extracted with DCM (2×40 mL) and the combined organic extracts were washed with sat. aq. $NaHCO_3$ (2×30 mL), and brine (2×30 mL), then dried over $Na_2SO_4$ and concentrated under reduced pressure, resulting in a crude product that was dissolved in THF (30 mL) and cooled to 0 °C. Morpholine (1.0 eq, 2.5 mmol, 0.22 g) was added and the mixture stirred for 1 h. The solvent was removed under reduced pressure. Water and ethyl acetate were added to the crude residue, which was then extracted with ethyl acetate (3×25 mL), washed with brine (2×20 mL), dried over $Na_2SO_4$, and concentrated under reduced pressure to yield a colorless oil (0.75 g, 2.5 mmol, 98%). $^1$H NMR (300 MHz, $CDCl_3$) $\delta$[ppm]=4.96–4.83 (m, 1H), 4.58–4.40 (m, 1H), 4.09 (q, J=7.1 Hz, 1H), 3.70 (s, 3H), 3.69–3.61 (m, 4H), 3.41–3.28 (m, 4H), 2.01 (s, 1H), 1.76 (d, $J$=12.8 Hz, 1H), 1.70–1.55 (m, 6H), 1.53–1.43 (m, 1H), 1.38–1.28 (m, 1H), 1.28–1.10 (m, 4H), 1.02–0.75 (m, 2H). $^{13}$C NMR (75 MHz, $CDCl_3$) $\delta$[ppm]=175.1, 157.4, 66.5, 52.3, 51.6, 44.1, 40.4, 34.2, 33.6, 32.7, 26.4, 26.2, 26.1, 21.1, 14.3. $[\alpha]_D^{22}=+16°$. MP=105–106 °C.

### (4-Morpholine-1-carbonyl)-L-cyclohexylalanine (42)

**42** was prepared according to procedure D using **41** (1.0 eq, 0.7 g, 2.4 mmol), resulting in a colorless solid (0.65 g, 2.3 mmol, 97%).$^1$H NMR (300 MHz, $CDCl_3$) $\delta$[ppm]=9.37 (s, 1H), 5.27–5.07 (m, 1H), 4.41 (s, 1H), 3.75–3.55 (m, 4H), 3.46–3.28 (m, 4H), 1.83–1.47 (m, 6H), 1.44–1.30 (m, 1H), 1.26–1.04 (m, 4H), 1.04–0.79 (m, 2H). $^{13}$C NMR (75 MHz, $CDCl_3$) $\delta$[ppm]=176.9, 158.1, 66.5, 51.9, 44.2, 39.6, 34.3, 33.6, 32.6, 26.6, 26.2, 26.1. 176.9, 158.1, 66.5, 51.9, 44.2, 39.6, 34.3, 33.6, 32.6, 26.5, 26.2, 26.1. $[\alpha]_D^{22}=+20°$. MP=96–97 °C.

## Inhibitor preparation

### *N*-((*S*)-1-(((*S,E*)-1-Fluoro-5-phenyl-1-(phenylsulfonyl)pent-1-en-3-yl)amino)-1-oxo-3-phenylpropan-2-yl)-4-methylpiperazine-1-carboxamide (1 a)

**1 a** was published previously and provided in form of a colorless solid. For experimental data, see Schirmeister et al.[45]

### Phenyl (*S,E*)-1-fluoro-3-((*S*)-2- (4-methylpiperazine-1-carboxamido)-3-phenylpropan-amido)-5-phenylpent-1-ene-1-sulfonate (1 b)

**1 b** was published previously and provided in form of a colorless solid. For experimental date see Jung, Fuchs et al.[49]

### *tert*-Butyl 4-(((*S*)-1-(((*S,E*)-1-fluoro-5-phenyl-1-(phenylsulfonyl)pent-1-en-3-yl)amino)-1-oxo-3-phenylpropan-2-yl)carbamoyl)piperazine-1-carboxylate (2 a)

**2 a** was prepared as published previously[46] according to procedure B using **17** (0.70 mmol, 0.25 g) and **22** (0.84 mmol, 0.30 g). Purification via HPLC resulted in a colorless solid (0.15 g, 0.22 mmol,

32%). $^1$H NMR (300 MHz, DMSO-$d_6$) $\delta$[ppm] = 8.24 (d, $J$ = 7.7 Hz, 1H), 7.98–7.90 (m, 2H), 7.89–7.77 (m, 1H), 7.79–7.67 (m, 2H), 7.31–7.12 (m, 8H), 7.13–7.05 (m, 2H), 6.66 (d, $J$ = 8.2 Hz, 1H), 6.26 (dd, $J_{H\text{-}F}$ = 33.9 Hz, $J_{H\text{-}H}$ = 8.9 Hz, 1H), 4.51 (t, $J$ = 7.8 Hz, 1H), 4.28 (td, $J$ = 8.8, 5.6 Hz, 1H), 3.23 (dd, $J$ = 9.5, 5.4 Hz, 8H), 2.99–2.70 (m, 2H), 1.99–1.64 (m, 2H), 1.39 (s, 9H). $^{13}$C NMR (75 MHz, DMSO-$d_6$) $\delta$[ppm] = 172.4, 157.4, 154.3, 141.3, 138.8, 137.1, 135.7, 130.6, 129.7, 128.8, 128.7, 128.6, 128.4, 126.6, 126.4, 119.8, 79.5, 56.4, 44.2, 43.8, 37.8, 35.5, 31.5, 28.5. $[\alpha]_D^{22} = -16°$. MP = 87–89 °C. ESI-MS: [M + H$^+$] calc. 679.2, found 679.1. Purity: 99%.

### 4-(((*S*)-1-(((*S,E*)-1-Fluoro-5-phenyl-1-(phenylsulfonyl)pent-1-en-3-yl)amino)-1-oxo-3-phenylpropan-2-yl)carbamoyl)piperazin-1-ium chloride (2 b)

**2 b** was published previously and provided in form of a colorless solid. For experimental date see Jung, Fuchs et al.[49]

### *N*-((*S*)-1-(((*S,E*)-1-Fluoro-5-phenyl-1-(phenylsulfonyl)pent-1-en-3-yl)amino)-1-oxo-3-phenylpropan-2-yl) morpholine-4-carboxamide (2 c)

**2 c** was prepared according to procedure B using **17** (0.70 mmol, 0.25 g) and **24** (0.84 mmol, 0.23 g). Purification via HPLC resulted in a colorless solid (0.15 g, 0.26 mmol, 37%). $^1$H NMR (300 MHz, DMSO-$d_6$) $\delta$[ppm] = 8.25 (d, $J$ = 7.7 Hz, 1H), 8.00–7.90 (m, 2H), 7.89–7.79 (m, 1H), 7.78–7.66 (m, 2H), 7.30–7.13 (m, 8H), 7.15–7.05 (m, 2H), 6.62 (d, $J$ = 8.1 Hz, 1H), 6.26 (dd, $J_{H\text{-}F}$ = 33.9 Hz, $J_{H\text{-}H}$ = 8.9 Hz, 1H), 4.61–4.42 (m, 1H), 4.36–4.16 (m, 1H), 3.57–3.39 (m, 4H), 3.29–3.13 (m, 4H), 2.98–2.72 (m, 2H), 2.58–2.38 (m, $J$ = 2.8, 2.4 Hz, 2H), 1.99–1.64 (m, 2H). $^{13}$C NMR (75 MHz, DMSO-$d_6$) $\delta$[ppm] = 172.8, 158.1, 155.8, 141.7, 139.2, 137.5, 136.0, 130.9, 130.1, 129.1, 129.0, 128.8, 127.0, 126.8, 120.1, 66.7, 56.8, 44.8, 44.6, 41.2, 38.1, 35.8, 31.8. $[\alpha]_D^{22} = -10°$. MP = 95–97 °C. ESI-MS: [M + H$^+$] calc. 580.2, found 580.0. Purity: 100%.

### *N*-((*S*)-1-(((*S,E*)-1-Fluoro-5-phenyl-1-(phenylsulfonyl)pent-1-en-3-yl)amino)-1-oxo-3-phenylpropan-2-yl)isonicotinamide (2 d)

**2 d** was published previously and provided in form of a colorless solid. For experimental date see Jung, Fuchs et al.[49]

### *N*-((*S*)-1-(((*S,E*)-1-Fluoro-5-phenyl-1-(phenylsulfonyl)pent-1-en-3-yl)amino)-1-oxo-3-phenylpropan-2-yl)thiophene-3-carbrboxamide (2 e)

**2 e** was prepared according to procedure B using **17** (0.70 mmol, 0.25 g) and **28** (0.84 mmol, 0.23 g). Purification via HPLC resulted in a colorless solid (0.090 g, 0.16 mmol, 22%). $^1$H NMR (300 MHz, DMSO-$d_6$) $\delta$[ppm] = 8.51–8.37 (m, 2H), 8.17 (ddd, $J$ = 6.5, 3.0, 1.3 Hz, 1H), 7.99–7.85 (m, 2H), 7.87–7.76 (m, 1H), 7.77–7.60 (m, 2H), 7.59–7.44 (m, 2H), 7.36–7.00 (m, 10H), 6.32 (ddd, $J_{H\text{-}F}$ = 33.7 Hz, 24.5 Hz, $J_{H\text{-}H}$ = 9.0 Hz, 1H), 4.77–4.36 (m, 2H), 3.14–2.82 (m, 2H), 2.45–2.31 (m, 2H), 2.01–1.64 (m, 2H). $^{13}$C NMR (75 MHz, DMSO-$d_6$) $\delta$[ppm] = 171.5, 162.4, 141.2, 138.5, 137.7, 137.0, 135.7, 130.6, 130.5, 129.6, 128.7, 128.6, 128.6, 127.5, 127.0, 126.8, 126.4, 119.6, 55.2, 44.4, 37.8, 31.5. $[\alpha]_D^{22} = -21°$. MP = 136–138 °C. ESI-MS: [M + H$^+$] calc. 577.2, found 577.2. Purity: 100%.

### *tert*-Butyl 4-(((*S*)-1-(((*S,E*)-1-fluoro-1-(phenoxysulfonyl)-5-phenylpent-1-en-3-yl)amino)-1-oxo-3-phenylpropan-2-yl)carbamoyl)piperazine-1-carboxylate (3 a)

**3 a** was prepared according to procedure B using **18** (0.67 mmol, 0.25 g) and **22** (0.81 mmol, 0.29 g). Purification via HPLC resulted in a colorless solid (0.18 g, 0.26 mmol, 43%). $^1$H NMR (300 MHz, DMSO-$d_6$) $\delta$[ppm] = 8.17 (d, $J$ = 7.6 Hz, 1H, *NH*), 7.54–7.44 (m, 2H), 7.43–7.35 (m, 1H), 7.34–7.10 (m, 12H), 6.68 (d, $J$ = 8.2 Hz, 1H, *NH*), 6.03 (dd, $J_{H\text{-}F}$ = 33.3 Hz, $J_{H\text{-}H}$ = 9.0 Hz, 1H), 4.56 (q, $J$ = 7.8 Hz, 1H), 4.28 (td, $J$ = 8.8, 5.9 Hz, 1H), 3.28–3.08 (m, 8H), 2.99–2.70 (m, 2H), 2.51–2.37 (m, 2H), 1.90–1.65 (m, 2H), 1.39 (s, 9H). $^{13}$C NMR (75 MHz, DMSO-$d_6$) $\delta$[ppm] = 172.6, 157.5, 154.3, 149.2, 141.2, 138.7, 130.9, 129.7, 128.8, 128.7, 128.4, 126.6, 126.4, 124.0, 122.5, 79.5, 56.4, 44.3, 43.8, 37.8, 34.9, 31.3, 28.5. $[\alpha]_D^{22} = -18°$. MP = 107–109 °C. ESI-MS: [M + H$^+$] calc. 639.2, found 639.1. Purity: 99%.

### 4-(((*S*)-1-(((*S,E*)-1-Fluoro-1-(phenoxysulfonyl)-5-phenylpent-1-en-3-yl)amino)-1-oxo-3-phenylpropan-2-yl)carbamoyl)piperperazin-1-ium chloride (3 b)

**3 b** was prepared according to procedure C using **3 a** (0.23 mmol, 0.16 g). Purification via HPLC resulted in a colorless solid (0.14 g, 0.22 mmol, 96%). $^1$H NMR (300 MHz, DMSO-$d_6$) $\delta$[ppm] = 9.29 (s, 2H), 8.40 (d, $J$ = 7.4 Hz, 1H), 7.53–7.43 (m, 2H), 7.42–7.35 (m, 1H), 7.34–7.12 (m, 12H), 7.06–6.96 (m, 1H), 6.03 (dd, $J_{H\text{-}F}$ = 33.3 Hz, $J_{H\text{-}H}$ = 9.0 Hz, 1H), 4.65–4.46 (m, 1H), 4.37–4.17 (m, 1H), 3.62–3.44 (m, 4H), 3.12–2.76 (m, 4H), 2.50–2.35 (m, 2H), 1.91–1.63 (m, 2H). $^{13}$C NMR (75 MHz, DMSO-$d_6$) $\delta$[ppm] = 172.5, 157.2, 149.2, 145.4, 141.3, 138.7, 130.9, 129.7, 128.8, 128.7, 128.5, 126.7, 126.4, 124.0, 122.4, 56.7, 44.5, 42.9, 41.1, 37.9, 34.9, 31.4. $[\alpha]_D^{22} = -16°$. MP = 125–127 °C. ESI-MS: [M + H$^+$] calc. 595.2, found 595.1. Purity: 98%.

### Phenyl (*S,E*)-1-fluoro-3-((*S*)-2-(morpholine-4-carboxamido)-3-phenylpropanamido)-5-phenylpent-1-ene-1-sulfonate (3 c)

**3 c** was prepared according to procedure B using **18** (0.40 mmol, 0.15 g) and **24** (0.48 mmol, 0.13 g). Purification via HPLC resulted in a colorless solid (0.14 g, 0.24 mmol, 59%). $^1$H NMR (300 MHz, DMSO-$d_6$) $\delta$[ppm] = 8.18 (d, $J$ = 7.6 Hz, 1H, *NH*), 7.54–7.43 (m, 3H), 7.43–7.35 (m, 2H), 7.36–7.10 (m, 10H), 6.64 (d, $J$ = 8.2 Hz, 1H, *NH*), 6.03 (dd, $J_{H\text{-}F}$ = 33.3 Hz, $J_{H\text{-}H}$ = 9.0 Hz, 1H), 4.58 (p, $J$ = 7.7 Hz, 1H), 4.29 (td, $J$ = 8.7, 5.9 Hz, 1H), 3.54–3.40 (m, 4H), 3.31–3.13 (m, 4H), 2.97–2.76 (m, 2H), 2.55–2.38 (m, 2H), 1.88–1.65 (m, 2H). $^{13}$C NMR (75 MHz, DMSO-$d_6$) $\delta$[ppm] = 172.6, 157.7, 149.3, 149.2, 145.4, 141.2, 138.7, 130.9, 129.7, 128.8, 128.7, 128.4, 126.6, 126.4, 124.0, 122.5, 122.4, 66.3, 56.4, 44.4, 40.8, 37.8, 34.9, 31.3. $[\alpha]_D^{22} = -12°$. ESI-MS: [M + H$^+$] calc. 596.2, found 596.1. Purity: 97%.

### Phenyl (*S,E*)-1-fluoro-3-((*S*)-2-(isonicotinamido)-3-phenylpropanamido)-5-phenylpent-1-ene-1-sulfonate (3 d)

**3 d** was published previously and provided in form of a colorless solid. For experimental date see Jung, Fuchs et al.[49]

### Phenyl (*S,E*)-1-fluoro-5-phenyl-3-((*S*)-3-phenyl-2-(thiophene-3-carboxamido)propanamido)pent-1-ene-1-sulfonate (3 e)

**3 e** was prepared according to procedure B using **18** (0.40 mmol, 0.15 g) and **28** (0.48 mmol, 0.13 g). Purification via HPLC resulted in a colorless solid (0.14 g, 0.24 mmol, 59%). $^1$H NMR (300 MHz, DMSO-$d_6$) $\delta$[ppm] = 8.53–8.39 (m, 2H), 8.34 (d, $J$ = 7.6 Hz, 1H), 8.19 (ddd, $J$ = 11.6, 2.9, 1.3 Hz, 1H), 7.61–7.43 (m, 2H), 7.45–7.34 (m, 1H),

7.35–7.17 (m, 10H), 7.19–7.10 (m, 3H), 6.10 (dd, $J_{H\text{-}F}$ = 33.3 Hz, $J_{H\text{-}H}$ = 9.1 Hz, 1H), 4.81–4.46 (m, 2H), 3.13–2.86 (m, 2H), 2.47–2.32 (m, 2H), 1.99–1.60 (m, 2H). $^{13}$C NMR (75 MHz, DMSO-$d_6$) $\delta$[ppm] = 171.7, 171.6, 162.4, 162.2, 149.1, 141.2, 141.2, 138.4, 137.7, 130.9, 130.8, 129.6, 129.6, 128.8, 128.7, 128.6, 128.5, 127.5, 127.1, 126.8, 126.4, 123.9, 122.5, 55.0, 40.8, 39.2, 38.1, 26.8. $[\alpha]_D^{22} = -20°$. MP = 119–121 °C. ESI-MS: [M + H$^+$] calc. 593.2, found 593.2. Purity: 99 %.

### Phenyl (*S,E*)-3-((*S*)-2-benzamido-3-phenylpropanamido)-1-fluoro-5-phenylpent-1-ene-1-sulfonate (3 f)

**3 f** was prepared according to procedure B using **18** (0.40 mmol, 0.15 g) and **30** (0.48 mmol, 0.13 g). Purification via HPLC resulted in a colorless solid (0.025 g, 0.043 mmol, 11 %). $^1$H NMR (300 MHz, DMSO-$d_6$) $\delta$[ppm] = 8.68–8.57 (m, 1H, *NH*), 8.47–8.29 (m, 1H, *NH*), 7.90–7.76 (m, 2H), 7.60–7.04 (m, 20H), 6.25 (dd, $J_{H\text{-}F}$ = 15.4 Hz, $J_{H\text{-}H}$ = 9.2 Hz, 1H), 5.00–4.75 (m, 1H), 4.78–4.47 (m, 1H), 3.16–2.93 (m, 2H), 2.61–2.36 (m, 2H), 1.94–1.67 (m, 2H). $^{13}$C NMR (75 MHz, DMSO-$d_6$) $\delta$[ppm] = 171.7, 166.7, 149.2, 141.2, 138.5, 134.4, 134.3, 132.1, 131.8, 130.9, 130.8, 130.8, 129.6, 129.6, 128.8, 128.8, 128.7, 128.7, 128.6, 127.9, 127.9, 127.8, 126.8, 126.4, 123.9, 122.5, 55.4, 45.1, 39.2, 31.7, 31.4. $[\alpha]_D^{22} = -15°$. MP = 150–152 °C. ESI-MS: [M + H$^+$] calc. 587.2, found 587.0. Purity: 96 %.

### *N*-((*S*)-3-Cyclohexyl-1-(((*S,E*)-1-fluoro-5-phenyl-1-(phenylsulfonyl)pent-1-en-3-yl)amino)-1-oxopropan-2-yl)isonicotinamide (4 a)

**4 a** was prepared according to procedure B using **17** (0.32 mmol, 0.11 g) and **32** (0.39 mmol, 0.11 g), resulting in a colorless solid (0.052 g, 0.090 mmol, 28 %) after purification via HPLC. $^1$H NMR (300 MHz, DMSO-$d_6$) $\delta$[ppm] = 8.85–8.66 (m, 2H), 8.42 (d, $J$ = 7.8 Hz, 1H), 7.96–7.87 (m, 2H), 7.85–7.76 (m, 3H), 7.73–7.61 (m, 2H), 7.35–7.04 (m, 5H), 6.35 (dd, $J_{H\text{-}F}$ = 33.2 Hz, $J_{H\text{-}H}$ = 8.9 Hz, 1H), 4.52 (dt, $J$ = 15.1, 7.9 Hz, 2H), 2.97–2.83 (m, 2H), 1.98–1.77 (m, 2H), 1.77–1.49 (m, 8H), 1.43–1.20 (m, 3H), 1.12 (d, $J$ = 7.9 Hz, 2H). $^{13}$C NMR (75 MHz, DMSO-$d_6$) $\delta$[ppm] = 172.1, 165.3, 150.6, 141.4, 141.3, 137.0, 135.6, 130.5, 128.7, 128.6, 126.4, 122.0, 52.0, 40.8, 34.2, 33.5, 31.6, 26.5, 26.2, 26.1. $[\alpha]_D^{22} = -15°$. MP = 108–110 °C. ESI-MS: [M + H$^+$] calc. 578.2, found 578.2. Purity: 95 %.

### *N*-((*S*)-1-(((*S,E*)-1-Fluoro-5-phenyl-1-(phenylsulfonyl)pent-1-en-3-yl)amino)-4-methyl-1-oxopentan-2-yl)isonicotinamide (4 b)

**4 b** was prepared according to procedure B using **17** (0.32 mmol, 0.11 g) and **34** (0.39 mmol, 0.090 g), resulting in a colorless solid (0.045 g, 0.083 mmol, 26 %) after purification via HPLC. $^1$H NMR (300 MHz, DMSO-$d_6$) $\delta$[ppm] = 8.80–8.58 (m, 2H), 8.06–7.81 (m, 2H), 7.87–7.66 (m, 3H), 7.69–7.47 (m, 3H), 7.33–7.20 (m, 3H), 7.24–7.07 (m, 1H), 6.12 (d, $J$ = 10.4 Hz, 1H), 5.86 (dd, $J_{H\text{-}F}$ = 32.5 Hz, $J_{H\text{-}H}$ = 8.1 Hz, 1H), 4.70–4.54 (m, 1H), 4.43–4.11 (m, 1H), 2.84–2.40 (m, 2H), 2.17–1.76 (m, 2H), 1.73–1.48 (m, 2H), 1.53–1.32 (m, 1H), 1.05–0.64 (m, 6H). $^{13}$C NMR (75 MHz, DMSO-$d_6$) $\delta$[ppm] = 173.0, 166.9, 150.6, 142.4, 141.9, 140.8, 140.4, 137.9, 133.5, 129.4, 128.5, 127.8, 126.1, 122.0, 121.8, 121.1, 53.0, 47.1, 40.8, 35.9, 32.6, 24.6, 22.3. $[\alpha]_D^{22} = -13°$. MP = 90–92 °C. ESI-MS: [M + H$^+$] calc. 538.2, found 538.0. Purity: 99 %.

### *N*-((*S*)-1-(((*S,E*)-1-Fluoro-5-phenyl-1-(phenylsulfonyl)pent-1-en-3-yl)amino)-1-oxo-4-phenylbutan-2-yl)isonicotinamide (4 c)

**4 c** was prepared according to procedure B using **17** (0.28 mmol, 0.10 g) and **36** (0.34 mmol, 0.10 g), resulting in a diastereomeric mixture which was separated via HPLC to yield the pure compound with (*E*)-configuration as a colorless solid (0.043 g, 0.073 mmol, 26 %). $^1$H NMR (300 MHz,DMSO-$d_6$) $\delta$[ppm] = 8.96–8.50 (m, 2H), 8.40 (d, $J$ = 7.9 Hz, 1H), 7.96–7.41 (m, 6H), 7.41–6.69 (m, 11H), 6.39 (dd, $J_{H\text{-}F}$ = 34.0 Hz, $J_{H\text{-}H}$ = 8.9 Hz, 1H), 4.69–4.12 (m, 2H), 3.59–3.07 (m, 2H), 2.77–2.50 (m, 2H), 2.14–1.70 (m, 2H). $^{13}$C NMR (75 MHz, DMSO-$d_6$) $\delta$[ppm] = 171.9, 166.0, 151.1, 142.1, 136.1, 131.0, 129.2, 126.8, 122.5, 120.0, 106.9, 70.3, 44.8, 34.0, 32.8, 30.1. $[\alpha]_D^{22} = -19°$. MP = 85–87 °C. ESI-MS: [M + H$^+$] calc. 586.2, found 586.2. Purity: 95 %.

### *N*-((*S*)-1-(((*S,E*)-1-Fluoro-5-phenyl-1-(phenylsulfonyl)pent-1-en-3-yl)amino)-3-(1H-indol-3-yl)-1-oxopropan-2-yl)isonicotinamide (4 d)

**4 d** was prepared according to procedure B using **17** (0.28 mmol, 0.10 g) and **38** (0.34 mmol, 0.11 g), resulting in a colorless solid (0.054 g, 0.088 mmol, 31 %) after purification via HPLC. $^1$H NMR (300 MHz, $CDCl_3$) $\delta$[ppm] = 10.73 (t, $J$ = 3.4 Hz, 1H), 8.89–8.73 (m, 1H), 8.73–8.55 (m, 2H), 8.51–8.32 (m, 1H), 8.01–7.47 (m, 8H), 7.32–6.80 (m, 9H), 6.31 (ddd, $J_{H\text{-}F}$ = 33.8 Hz, $J_{H\text{-}F}$ = 8.9, 4.7 Hz, 1H), 4.73–4.56 (m, 1H), 4.50 (q, $J$ = 8.1 Hz, 1H), 3.22–2.99 (m, 2H), 2.85–2.38 (m, 2H), 2.05–1.52 (m, 2H). $^{13}$C NMR (75 MHz, $CDCl_3$) $\delta$[ppm] = 172.0, 168.6, 150.9, 141.6, 139.4, 138.6, 137.3, 133.6, 129.6, 128.4, 128.2, 127.6, 126.0, 123.9, 123.0, 122.8, 121.6, 121.2, 119.1, 118.8, 117.8, 116.8, 113.1, 110.1, 54.7, 47.0, 37.4, 32.4, 28.4. $[\alpha]_D^{22} = -21°$. MP = 101–103 °C. ESI-MS: [M + H$^+$] calc. 611.2, found 611.2. Purity: 96 %.

### Phenyl (*S,E*)-3-((S)-3-cyclohexyl-2-(isonicotinamido) propanamido)-1-fluoro-5-phenylpent-1-ene-1-sulfonate (5 a)

**5 a** was prepared according to procedure B using **18** (0.27 mmol, 0.10 g) and **32** (0.32 mmol, 0.088 g), resulting in a colorless solid (0.038 g, 0.064 mmol, 24 %) after purification via HPLC. $^1$H NMR (300 MHz, DMSO-$d_6$) $\delta$[ppm] = 8.89–8.71 (m, 2H), 8.44 (m, 1H), 7.96–7.87 (m, 2H), 7.87–7.79 (m, 3H), 7.77–7.66 (m, 2H), 7.41–7.09 (m, 5H), 6.40 (dd, $J_{H\text{-}F}$ = 33.1 Hz, $J_{H\text{-}H}$ = 9.0 Hz, 1H), 4.58 (dt, $J$ = 15.2, 7.9 Hz, 2H), 2.99–2.88 (m, 2H), 2.00–1.80 (m, 2H), 1.78–1.48 (m, 8H), 1.48–1.25 (m, 3H), 1.16 (d, $J$ = 7.9 Hz, 2H). $^{13}$C NMR (75 MHz, DMSO-$d_6$) $\delta$[ppm] = 172.2, 165.5, 150.9, 141.5, 141.4, 137.2, 135.9, 130.6, 128.9, 128.8, 126.7, 122.5, 52.4, 41.2, 34.6, 33.9, 32.0, 26.6, 26.3, 26.0. $[\alpha]_D^{22} = -12°$. MP = 123–125 °C. ESI-MS: [M + H$^+$] calc. 594.2, found 594.2. Purity: 99 %.

### Phenyl (*S,E*)-1-fluoro-3-((*S*)-2-(isonicotinamido)-4-methylpentanamido)-5-phenylpent-1-ene-1-sulfonate (5 b)

**5 b** was prepared according to procedure B using **18** (0.25 mmol, 0.093 g) and **34** (0.30 mmol, 0.071 g), resulting in a colorless solid (0.031 g, 0.056 mmol, 22 %) after purification via HPLC. $^1$H NMR (300 MHz, $CDCl_3$) $\delta$[ppm] = 8.81 (d, $J$ = 8.4 Hz, 1H), 8.73 (s, 2H), 8.36 (dd, $J$ = 14.8, 8.0 Hz, 1H), 7.80 (d, $J$ = 7.5 Hz, 2H), 7.54–7.36 (m, 2H), 7.35–7.08 (m, 7H), 7.01 (d, $J$ = 7.5 Hz, 1H), 6.15 (dd, $J_{H\text{-}F}$ = 32.4 Hz, $J_{H\text{-}H}$ = 8.8 Hz, 1H), 4.89 (s, 1H), 4.69–4.31 (m, 1H), 1.67 (s, 2H), 1.10–0.58 (m, 11H). $^{13}$C NMR (75 MHz, $CDCl_3$) $\delta$[ppm] = 173.0, 166.9, 150.6, 147.8, 147.7, 141.9, 140.8, 136.8, 134.8, 131.2, 131.1, 129.3, 128.5, 126.8, 126.1, 122.4, 121.1, 53.0, 47.1, 40.8, 35.9, 32.6, 24.6, 22.3. $[\alpha]_D^{22} = -20°$. MP = 76–78 °C. ESI-MS: [M + H$^+$] calc. 554.2, found 554.0. Purity: 99 %.

### Phenyl (*S,E*)-1-fluoro-3-((*S*)-2-(isonicotinamido)-4-phenylbutanamido)-5-phenylpent-1-ene-1-sulfonate (5 c)

**5 c** was prepared according to procedure B using **18** (0.40 mmol, 0.15 g) and **36** (0.48 mmol, 0.18 g), resulting in a colorless solid

(0.060 g, 0.10 mmol, 25%) after purification via HPLC. $^1$H NMR (300 MHz, $CDCl_3$) $\delta$[ppm] = 9.02 (dd, $J$ = 7.6, 5.4 Hz, 1H), 8.88 (t, $J$ = 5.3 Hz, 2H), 8.53 (d, $J$ = 7.9 Hz, 1H), 8.09–7.82 (m, 5H), 7.86–7.66 (m, 2H), 7.51–7.09 (m, 10H), 6.51 (ddd, $J_{H\text{-}F}$ = 33.9 Hz, $J_{H\text{-}F}$ = 8.9, 5.1 Hz, 1H), 4.83–4.34 (m, 2H), 2.86–2.68 (m, 4H), 2.33–1.81 (m, 4H). $^{13}$C NMR (75 MHz, $CDCl_3$) $\delta$[ppm] = 172.2, 166.3, 151.6, 142.2, 136.5, 131.4, 129.5, 127.0, 122.9, 120.4, 107.3, 70.4, 44.9, 34.3, 32.8, 30.3. $[\alpha]_D^{22} = -15°$. MP = 96–98 °C. ESI-MS: [M + H$^+$] calc. 602.2, found 602.2. Purity: 99%.

### Phenyl (*S,E*)-3-((*S*)-3-(1H-indol-3-yl)-2-(isonicotinamido) propanamido)-1-fluoro-5-phenylpent-1-ene-1-sulfonate (5 d)

**5 d** was prepared according to procedure B using **18** (0.54 mmol, 0.20 g) and **38** (0.65 mmol, 0.20 g), resulting in a colorless solid (0.071 g, 0.11 mmol, 20%) after purification via HPLC. $^1$H NMR (300 MHz, $CDCl_3$) $\delta$[ppm] = 10.68–10.33 (m, 1H), 8.75–8.52 (m, 1H), 8.50–8.35 (m, 2H), 8.22 (d, $J$ = 8.5 Hz, 1H), 7.79–7.51 (m, 4H), 7.52–7.36 (m, 5H), 7.09–6.67 (m, 9H), 6.12 (dd, $J_{H\text{-}F}$ = 33.9 Hz, $J_{H\text{-}H}$ = 8.9 Hz, 1H), 4.60–4.14 (m, 2H), 3.00–2.80 (m, 2H), 2.67–2.39 (m, 2H), 1.80–1.39 (m, 2H). $^{13}$C NMR (75 MHz, $CDCl_3$) $\delta$[ppm] = 172.0, 168.6, 150.9, 149.4, 141.6, 138.6, 137.3, 133.0, 132.9, 129.8, 128.4, 127.6, 127.3, 126.0, 123.9, 122.1, 121.6, 121.2, 119.1, 117.8, 117.0, 115.0, 113.1, 110.1, 54.7, 47.1, 47.0, 37.4, 32.4, 28.4. $[\alpha]_D^{22} = -22°$. MP = 114–116 °C. ESI-MS: [M + H$^+$] calc. 627.2, found 627.1. Purity: 96%.

### Phenyl (*S,E*)-3-((*S*)-2-(4-((*tert*-butoxycarbonyl)amino) benzamido)-3-cyclohexylpropanamido)-1-fluoro-5-phenylpent-1-ene-1-sulfonate (6 a)

**6 a** was prepared according to procedure B using **18** (0.54 mmol, 0.20 g) and **40** (0.65 mmol, 0.25 g), resulting in a diastereomeric mixture which was separated via HPLC to yield the pure compound with (*E*)-configuration as a colorless solid (0.25 g, 0.35 mmol, 65%) after purification via HPLC. $^1$H NMR (300 MHz, DMSO-$d_6$) $\delta$[ppm] = 9.60 (d, $J$ = 2.6 Hz, 1H), 8.40–8.10 (m, 2H), 7.94–7.70 (m, 2H), 7.61–7.34 (m, 4H), 7.35–7.05 (m, 6H), 7.00 (d, $J$ = 7.2 Hz, 2H), 6.15 (dd, $J_{H\text{-}F}$ = 33.2 Hz, $J_{H\text{-}H}$ = 9.0 Hz, 1H), 4.95–4.81 (m, 1H), 4.66–4.38 (m, 1H), 2.61–2.32 (m, 2H), 1.85–1.52 (m, 8H), 1.48 (s, 9H), 1.28–1.02 (m, 3H), 1.04–0.73 (m, 2H). $^{13}$C NMR (75 MHz, DMSO-$d_6$) $\delta$[ppm] = 166.3, 153.1, 142.9, 141.2, 130.9, 128.9, 128.8, 128.7, 127.8, 122.4, 117.5, 79.9, 34.3, 32.4, 31.5, 28.5, 26.5, 26.1. $[\alpha]_D^{22} = -15°$. MP = 118–120 °C. ESI-MS: [M + Na$^+$] calc. 730.2, found 730.2. Purity: 97%.

### 4-(((*S*)-3-Cyclohexyl-1-(((*S,E*)-1-fluoro-1-(phenoxysulfonyl)-5-phenylpent-1-en-3-yl)amino)-1-oxopropan-2-yl)carbamoyl) benzenaminium chloride (6 b)

**6 b** was prepared according to procedure C using **6 a** (0.35 mmol, 0.25 g). Purification via HPLC resulted in a diastereomeric mixture which was separated via HPLC to yield the pure compound with (*E*)-configuration as a colorless solid (0.17 g, 0.26 mmol, 74%). $^1$H NMR (300 MHz, DMSO-$d_6$) $\delta$[ppm] = 8.56–8.19 (m, 4H), 8.06–7.72 (m, 2H), 7.61–7.07 (m, 10H), 7.07–6.90 (m, 2H), 6.45 (dd, $J$ = 21.8, 10.0 Hz, 1H), 6.14 (dd, $J_{H\text{-}F}$ = 33.3 Hz, $J_{H\text{-}H}$ = 9.1 Hz, 1H), 5.06–4.72 (m, 1H), 4.66–4.35 (m, 1H), 2.63–2.34 (m, 2H), 2.34–2.09 (m, 2H), 1.98–1.43 (m, 6H), 1.45–0.99 (m, 3H), 1.04–0.73 (m, 2H). $^{13}$C NMR (75 MHz, DMSO-$d_6$) $\delta$[ppm] = 172.7, 166.0, 149.2, 141.2, 130.9, 129.6, 128.8, 128.7, 126.4, 122.4, 120.1, 66.8, 34.3, 33.59, 32.4, 31.5, 26.5, 26.2, 26.1. $[\alpha]_D^{22} = -9°$. MP = 130–132 °C. ESI-MS: [M + H$^+$] calc. 607.3, found 607.2. Purity: 95%.

### Phenyl (*S,E*)-3-((*S*)-3-cyclohexyl-2-(morpholine-4-carbox-amido)propanamido)-1-fluoro-5-phenylpent-1-ene-1-sulfonate (6 c)

**6 c** was prepared according to procedure B using **18** (0.08 mmol, 0.030 g) and **42** (0.08 mmol, 23 mg), resulting in a colorless solid (5.5 mg, 0.009 mmol, 9%) after purification via HPLC. $^1$H NMR (600 MHz, DMSO-$d_6$) $\delta$[ppm] = 8.32 (s, 1H), 8.15 (d, $J$ = 7.7 Hz, 1H), 7.52–7.37 (m, 3H), 7.33–7.11 (m, 5H), 6.51 (d, $J$ = 7.9 Hz, 1H), 6.11 (dd, $J$ = 33.3, 9.0 Hz, 1H), 4.61–4.52 (m, 1H), 4.17–4.08 (m, 1H), 3.60–3.46 (m, 4H), 3.33–3.22 (m, 4H), 1.88–1.71 (m, 2H), 1.71–1.55 (m, 4H), 1.53–1.36 (m, 3H), 1.30–1.21 (m, 2H), 1.19–1.06 (m, 4H), 0.95–0.75 (m, 3H). $^{13}$C NMR (151 MHz, DMSO-$d_6$) $\delta$[ppm] = 173.2, 157.5, 148.7, 147.8, 145.9, 140.9, 130.5, 126.0, 123.6, 122.0, 79.2, 66.0, 52.0, 44.1, 43.78, 34.5, 33.7, 33.2, 32.0, 30.9, 26.1, 25.8, 25.7. $[\alpha]_D^{22} = -2°$. MP = 116–117 °C. ESI-MS: [M + Na$^+$] calc. 601.3, found 601.2. Purity: 95%.

### *Molecular docking*

Since the inhibitors were designed to react covalently with cysteine-25 of CatS, two different docking approaches were followed. First, a conventional non-covalent docking was performed, to estimate affinity and geometry of the pre-organized enzyme-inhibitor complex, secondly a covalent docking was used to determine the final covalent enzyme-inhibitor complex. In both docking setups a crystallographic reference ligand was used for validation via redocking (Table A, Supporting Information). Molecular docking experiments were performed using the following crystal structure freely available in the protein data bank (PDB):[55] Cathepsin S covalently bound to *N*-2-(morpholin-4-ylcarbonyl)-*N*-[(3*S*)-1-phenyl-5-(phenylsulfonyl)pentan-3-yl]-l-leucinamide (C1P), PDB entry 1NPZ.[29] For both docking approaches, chain A of the dimer of 1NPZ was extracted via PyMOL 2.5.2.[56] All ligands were energetically minimized prior docking with Molecular operating environment (MOE Version 2020.09)[57] using the MMF94x force field.[58] For visual presentation of the top binding poses, PyMOL 2.5.2 was used.[56]

### Docking approach A: non-covalent docking with LeadIT

The non-covalent docking was performed with LeadIT 2.3.2.[59] The receptors were prepared in MOE with the protonate3D functionality and the covalent bond between the co-crystallized ligand and the corresponding protease was untethered via the Builder tool in MOE. For the receptor the binding site was defined as a 6.5 Å shell around the bound reference ligand. Water molecules that form at least three hydrogen bonds with the receptor and ligand were kept as part of the binding site. The docking was performed under default settings using the enthalpy-entropy hybrid approach with 2,000 solutions per iteration and fragmentation. Only the top pose of the initial docking was kept and re-scored using the HYDE scoring function.[60] For the docking, pharmacophore constraints needed to be included to obtain reasonable binding modes. The nitrogen atoms of the peptide backbone were therefore defined as H-bond donors with a 1 Å sphere radius.

### Docking approach B: covalent docking with MOE

Covalent docking was performed with MOE. The receptor was prepared using the 3D protonation tool inside MOE. For the covalent reaction of the different warheads, the already existing template reactions were used. Initial 30 poses from the triangle match placement with London △G scoring were re-scored using the Affinity △G scoring function and induced fit refinement

implemented in MOE. 10 Poses were kept and visually inspected for binding geometry the interactions matching between the docked inhibitor pose and co-crystallized ligand with the enzyme. The poses best matching inspected interaction patterns are further discussed.

### Fluorometric enzyme assay

#### *Cathepsin S*

#### Assay procedure

The assay was modified after Brömme et al.[50] The fluorescence increase upon cleavage of the fluorogenic substrate *Z*-Val-Val-Arg-AMC by Cathepsin S (CatS) was monitored by a Tecan Spark fluorimeter (δ excitation: 365 nm, δ emission: 460 nm; Tecan Group, Switzerland). CatS (recombinant from *E. coli*, SigmaAldrich, Germany) was incubated with enzyme buffer (35 mM potassium phosphate, 35 mM sodium acetate, 2 mM DTT, 2 mM EDTA, pH 6.5) at room temperature for 20–30 min. Assay buffer (50 mM $KH_2PO_4$, 50 mM $K_2HPO_4$, 2.5 mM DTT, 2.5 mM EDTA, pH 6.5) was mixed with 1–5 nM CatS in enzyme buffer, followed by inhibitor in DMSO or DMSO (negative control), and 10 μM substrate *Z*-Val-Val-Arg-AMC (Bachem, Switzerland). Black, flat-bottom 96-well microtiter plates (Greiner Bio-One, Germany) were used. Inhibitor screening concentrations started at 20 μM, followed by 1 μM, 200 nM, and 50 nM.

#### $K_M$ determination

The assay was performed as described above using different concentrations of *Z*-Val-Val-Arg-AMC (3.125 μM, 6.25 μM, 12.5 μM, 25 μM, 50 μM) and Z-Phe-Arg-AMC (0.41 μM, 1.2 μM, 3.7 μM, 11 μM, 33 μM, 60 μM, 100 μM). GraFit (version 5.0.13, 2006, Erithracus Software Ltd., UK)[61] was used for data analysis and non-linear regression. The $K_M$ value was calculated as described by Michaelis-Menten [Equation (2), $K_M$ = 34 μM for Z-Val-Val-Arg-AMC; $K_M$ = 35 μM for Z-Phe-Arg-AMC]:

$$v_0 = \frac{v_{max} \cdot [S]}{K_M + [S]} \tag{2}$$

in which $v_0$ = initial velocity; $v_{max}$ = maximal velocity; [S] = substrate concentration.

The graphs are shown in the Supporting Information.

#### $IC_{50}$ and $K_i$ calculations

GraFit (version 5.0.13, 2006, Erithracus Software Ltd., UK) was used for data analysis and non-linear regression.[61]

For compounds without a time-dependent mode of inhibition (fluorinated vinylsulfones as inhibitors of CatS, CatB, CatL; fluorinated vinylsulfonates as inhibitors of CatB, CatL), the residual enzyme activity in % was plotted against the inhibitor concentration in μM. Then, $IC_{50}$ values were obtained by non-linear regression [Equation (3)]:

$$v_i = \frac{v_0}{1 + \left(\frac{[I]}{IC_{50}}\right)^S} \tag{3}$$

in which $v_0$ = enzyme activity without inhibitor; $v_i$ = enzyme activity in presence of inhibitor; [I] = inhibitor concentration; S = slope factor.

$K_i$ values were calculated by using the Cheng-Prusoff equation to correct the $IC_{50}$ values to zero substrate concentration [Equation (4)]:[51]

$$K_i = \frac{IC_{50} \text{ or } K_i^{app}}{1 + \frac{[S]}{K_M}} \tag{4}$$

in which CatS: [S] = 10 μM, $K_M$ = 34 μM. CatB: [S] = 100 μM, $K_M$ = 150 μM. CatL: [S] = 6.25 μM, $K_M$ = 6.5 μM.

For compounds with a time-dependent mode of inhibition (fluorinated vinylsulfonates as inhibitors of CatS), the $K_i$ values were calculated as published previously for slow, tight binders [Equation (5)].[49]

$$E + I \underset{k_2}{\overset{k_1}{\rightleftharpoons}} E^{\cdots}I \underset{k_4}{\overset{k_3}{\rightleftharpoons}} E{-}I \tag{5}$$

in which E = enzyme; I = inhibitor, $k$ = reaction constant; E…I = non-covalent enzyme-inhibitor complex; E–I = covalent enzyme-inhibitor complex.

The initial ($v_i$) and steady-state ($v_s$) velocities in inhibitor presence and the pseudo-first order rate constants $k_{obs}$ were determined for different inhibitor concentrations. The progress curves were fitted to the slow-binding equation [Equation (6)]:[52]

$$[P] = v_s \cdot t + \frac{v_i - v_s}{k_{obs}} \cdot [1 - \exp(-k_{obs} \cdot t)] + off \tag{6}$$

in which $v_s$ = steady-state velocity, $v_i$ = initial velocity, off = offset.

Then, the $k_{obs}$ values were plotted against the inhibitor concentrations [I] with the following Equation (7):

$$k_{obs} = k_4 + \left(\frac{k_3 \cdot [I]}{K_i^{app} + [I]}\right) \tag{7}$$

in which $K_i^{app}$ determination using $k_{obs}$.

The resulting dissociation constant of the initial enzyme-inhibitor complex $K_i^{app}$ was then corrected to zero substrate concentration using the Cheng-Prusoff relationship (Equation 4), giving the $K_i$ value.[51]

### Dilution assay

Dilution assays were performed for selected compounds as published previously.[49] CatS (0.5 μM) in enzyme buffer (90 μL) was incubated for with inhibitors (10 μL in DMSO) for 30 min in concentrations corresponding to tenfold the $IC_{50}$ value obtained from the fluorometric enzyme assay ensuring complete inhibition. These mixtures (2 μL) were diluted 100-fold in assay buffer (198 μL) containing 5 μL substrate (400 μM) to give a final substrate concentration of 10 μM. Recovery of enzyme activity was measured immediately by fluorescence readout. CatS with DMSO and no inhibitor added was used as a reference while the irreversible inhibitor K11777 was used as an irreversible control.[53]

#### *Selectivity towards CatL and CatB[45,49]*

Cathepsin B (CatB, SigmaAldrich, Germany) and cathepsin L (CatL, Sigma-Aldrich, Germany) were incubated in enzyme buffer (50 mM Tris-HCl, 5 mM EDTA, 200 mM NaCl, 2 mM DTT, pH 6.5) at room temperature for 20–30 min. Assay buffer (50 mM Tris-HCl, 5 mM EDTA, 200 mM NaCl, 0.005% Brij35, pH 6.5) was mixed with CatB or CatL in enzyme buffer, then inhibitor in DMSO or DMSO (negative control) was added, followed by 100 μM (CatB) or 6.25 μM (CatL) substrate *Z*-Phe-Arg-AMC (Bachem, Switzerland). The enzyme activity was monitored by a Tecan Spark (Tecan Group, Switzerland) fluorescence reader using black Greiner flat-bottom 96-well microtiter plates (Greiner Bio-One GmbH, Germany). Inhibitor screening concentrations started at 20 μM, followed by 1 μM, and 200 nM if the percentual inhibition exceeded 50% for the previous inhibitor concentration. $IC_{50}$ values were determined for inhibitors with $>50\%$ inhibition at 20 μM.

### Cytotoxicity

#### *Cell culture*

The human cell line MDA-MB-231 from adenocarcinomic breast tissue was cultured at 37 °C and 5% $CO_2$ in Dulbeccos Modified Eagles Medium (DMEM, 4.5 g/L D-glucose, L-glutamine; Gibco by ThermoFisher Scientific, Germany), supplemented with 10% FBS (SigmaAldrich, Germany) and 1% Penicillin/Streptomycin (Invitrogen, Germany). Cells were cultured in a T75 culture flask and passaged two to three times per week using TrypLE™ Express (Gibco by ThermoFisher Scientific, Germany).

Murine bone marrow derived from C7BL/6 mice was seeded (2× 10 cells/mL) in untreated 12 well plates (Gibco by ThermoFisher Scientific, Germany) using Iscoves Modified Dulbecco's Medium, supplement with 5% FBS, 2 mM L-glutamine, 100 IU/mL penicillin, 100 μg/mL streptomycin and 50 μM $\beta$-mercaptoethanol (all components from Sigma-Aldrich, Germany) and 10 ng/mL GM-CSF (MILTENYI BIOTEC, Germany). Media was replenished on days 3 and 6 of culture.

### Cell viability assay

MDA-MB-231 cells were seeded at a density of 2,500 cells/well in a white half area 96-well plate (Greiner Bio-One, Germany) and incubated at 37 °C. 24 h after seeding, the medium was removed and cells were treated with 50 μL of either 100 μM or 20 μM solution of compounds **5a**, **5b**, **6b** and **3c** in fresh culture medium (0.1% DMSO) or culture medium (0.1% DMSO) only. For each condition, quadruplicates were performed. Cells were incubated for 24 h. After the treatment, CellTiter-Glo® Assay solution (50 $\mu$L) was added to each well, and the plate was placed on an orbital shaker for 2 minutes and subsequently incubated 10 minutes at room temperature. Luminescence readout was performed with a Promega GloMax®-Multi Detection System using the manufacturer's protocol.

#### *DC cytotoxicity*

On day 7 of DC culture, compounds (1 μM) and lipopolysaccharide (100 ng/mL) was applied as indicated. On the following day, samples were harvested, washed with buffer (PBS, 2% FBS, 2 mM EDTA) and preincubated with Fc receptor blocking rat-anti-mouse antibody (clone 2.4G2; ThermoFisher Scientific, Germany) to prevent unspecific antibody binding. Then, samples were incubated with phycoerythrin-labeled rat-anti-mouse CD11c antibody (clone N418; ThermoFisher Scientific, Germany) to delineate $CD11c^+$ DC, washed with PBS and incubated with allophycocyanin-eFluor780 tandem conjugate labeled fixable viability dye to detect dead cells within the $CD11c^+$ DC fraction. Fluorescence intensities were measured using an Attune NxT Flow Cytometer and were analyzed using Attune NxT software (both from ThermoFisher Scientific, Germany).

## Abbreviations

ACN, acetonitrile; AMC, 7-amino-4-methylcoumarin; APC, antigen-presenting cell; boc, tert-butyl carbamoyl; CatB, cathepsin B; CatL, cathepsin L; CatS, cathepsin S; CH, cyclohexane; compd, compound; cyAla, cyclohexylalanine; DC, dendritic cell; DCM, dichloromethane; DECP, diethyl chlorophosphate; DIPEA, *N,N*-diisopropylethylamine; DMF, dimethylformamide; EA, ethyl acetate; HOBt, 1-hydroxybenzotriazole; hPhe, homophenylalanine; HWE, Horner-Wadsworth-Emmons; KHMDS, potassium bis(trimethylsilyl)amide; LHMDS, lithium bis(trimethylsilyl)amide; Me, methyl; Pip, piperazine; SAR, structure-activity relationship; SI, selectivity index; TBTU, 2-(1*H*-benzotriazole-1-yl)-1,1,3,3-tetramethylaminium tetrafluoroborate; THF, tetrahydrofuran, Z/Cbz; benzyloxycarbonyl.

## Supporting Information

The supporting information includes molecular docking score tables, enzyme assay plots, and characterization data (LC–MS, NMR) and is available free of charge.

## *Acknowledgements*

*We acknowledge Ann-Katrin Fuchs, Albin Lahu, and Anna Riede (all at Johannes Gutenberg University Mainz) for their support in this project, as well as all other co-workers in the Q5 subproject of the CRC1066 (JGU Mainz, MPIP Mainz). Financial support by the Deutsche Forschungsgemeinschaft (DFG) in the framework of the CRC 1066 (Nanodimensional Polymeric Therapeutics for Tumor Therapy), project Q5 (Targeting and Immunomodulator Structures and their Coupling to Therapeutic Nanosystems for Oncological Application) is gratefully acknowledged. Open Access funding enabled and organized by Projekt DEAL.*

## *Conflict of Interests*

The authors declare no conflicts of interest.

## Data Availability Statement

The data that support the findings of this study are available in the supplementary material of this article.

**Keywords:** cathepsins · inhibitors · molecular docking · structure-activity relationship · tumor microenvironment

[1] V. Leroy, S. Thurairatnam, *Exp. Opin. Therap. Patents* **2005**, *14*, 301–311.
[2] H.-H. Otto, T. Schirmeister, *Chem. Rev.* **1997**, *97*, 133–171.
[3] H. Kirschke, B. Wiederanders, D. Brömme, A. Rinne, *Cathepsin S from Bovine Spleen. Biochem. J.* **1989**, *264*, 467–473.
[4] G. P. Shi, A. C. Webb, K. E. Foster, J. H. M. Knoll, C. A. Lemere, J. S. Munger, H. A. Chapman, *J. Biol. Chem.* **1994**, *269*, 11530–11536.
[5] D. Bararia, J. A. Hildebrand, S. Stolz, S. Haebe, S. Alig, C. P. Trevisani, F. Osorio-Barrios, M. D. Bartoschek, M. Mentz, A. Pastore, E. Gaitzsch, M. Heide, V. Jurinovic, K. Rautter, J. Gunawardana, M. B. Sabdia, M. Szczepanowski, J. Richter, W. Klapper, A. Louissaint, C. Ludwig, S. Bultmann, H. Leonhardt, S. Eustermann, K. P. Hopfner, W. Hiddemann, M. von Bergwelt-Baildon, C. Steidl, R. Kridel, J. W. D. Tobin, M. K. Gandhi, D. M. Weinstock, M. Schmidt-Supprian, M. B. Sárosi, M. Rudelius, V. Passerini, J. Mautner, O. Weigert, *Cell Rep.* **2020**, *31*, 107522.
[6] E. Dheilly, E. Battistello, N. Katanayeva, S. Sungalee, J. Michaux, G. Duns, S. Wehrle, J. Sordet-Dessimoz, M. Mina, J. Racle, P. Farinha, G. Coukos, D. Gfeller, A. Mottok, R. Kridel, B. E. Correia, C. Steidl, M. Bassani-Sternberg, G. Ciriello, V. Zoete, E. Oricchio, *Cancer Cell* **2020**, *37*, 674–689.e12.
[7] S. H. McDowell, S. A. Gallaher, R. E. Burden, C. J. Scott, *Biochim. Biophys. Acta Mol. Cell Res.* **2020**, *1867*, 118781.
[8] A. C. Da Costa, F. Santa-Cruz, L. A. R. Mattos, M. A. R. Aquino, C. R. Martins, Á. A. B. Ferraz, J. L. Figueiredo, *Mol. Clin. Oncol.* **2020**, *12*, 99–103.
[9] R. D. A. Wilkinson, A. Young, R. E. Burden, R. Williams, C. J. Scott, *Mol. Cancer* **2016**, *15*, 1–11.
[10] R. J. Riese, R. N. Mitchell, J. A. Villadangos, G. P. Shi, J. T. Palmer, E. R. Karp, G. T. De Sanctis, H. L. Ploegh, H. A. Chapman, *J. Clin. Invest.* **1998**, *101*, 2351–2363.
[11] J. A. Villadangos, R. J. Riese, C. Peters, H. A. Chapman, H. L. Ploegh, *J. Exp. Med.* **1997**, *186*, 549–560.
[12] R. J. Riese, P. R. Wolf, D. Brömme, L. R. Natkin, J. A. Villadangos, H. L. Ploegh, H. A. Chapman, *Immunity* **1996**, *4*, 357–366.
[13] S. Guo-Ping, J. A. Villadangos, G. Dranoff, C. Small, G. Lijuan, K. J. Haley, R. Riese, H. L. Ploegh, H. A. Chapman, *Immunity* **1999**, *10*, 197–206.
[14] C. Beers, A. Burich, M. J. Kleijmeer, J. M. Griffith, P. Wong, A. Y. Rudensky, *J. Immunol.* **2005**, *174*, 1205–1212.
[15] L. C. Hsing, A. Y. Rudensky, *Immunol. Rev.* **2005**, *207*, 229–241.
[16] T. Jakoš, A. Pišlar, A. Jewett, J. Kos, *Front. Immunol.* **2019**, *10*, 2037.
[17] B. Farhood, M. Najafi, K. Mortezaee, *J. Cell. Physiol.* **2019**, *234*, 8509–8521.
[18] V. Quaranta, M. C. Schmid, *Cells* **2019**, *8*, 747.
[19] C. Fu, A. Jiang, *Front. Immunol.* **2018**, *9*, 3059.
[20] X. Yan, C. Wu, T. Chen, M. M. Santos, C. L. Liu, C. Yang, L. Zhang, J. Ren, S. Liao, H. Guo, G. K. Sukhova, G. P. Shi, *Mol. Immunol.* **2017**, *82*, 66–74.
[21] W. L. Liu, D. Liu, K. Cheng, Y. J. Liu, S. Xing, P. D. Chi, X. H. Liu, N. Xue, Y. Z. Lai, L. Guo, G. Zhang, *Oncotarget* **2016**, *7*, 28124.
[22] Y. Yixuan, L. S. Kiat, C. L. Yee, L. Huiyin, C. Yunhao, C. P. Kuan, A. Hassan, W. T. Ting, S. T. Manuel, Y. K. Guan, L. Y. Pin, *J. Proteome Res.* **2010**, *9*, 4767–4778.
[23] R. E. Burden, J. A. Gormley, D. Kuehn, C. Ward, H. F. Kwok, M. Gazdoiu, A. McClurg, T. J. Jaquin, J. A. Johnston, C. J. Scott, S. A. Olwill, *Biochimie* **2012**, *94*, 487–493.
[24] R. E. Burden, J. A. Gormley, T. J. Jaquin, D. M. Small, D. J. Quinn, S. M. Hegarty, C. Ward, B. Walker, J. A. Johnston, S. A. Olwill, C. J. Scott, *Clin. Cancer Res.* **2009**, *15*, 6042–6051.
[25] N. Fuchs, M. Meta, D. Schuppan, L. Nuhn, T. Schirmeister, *Cells* **2020**, *9*, 2021.
[26] R. Bai, N. Chen, L. Li, N. Du, L. Bai, Z. Lv, H. Tian, J. Cui, *Front. Oncol.* **2020**, *10*, 1290.
[27] J. R. Somoza, H. Zhan, K. K. Bowman, L. Yu, K. D. Mortara, J. T. Palmer, J. M. Clark, M. E. McGrath, *Biochemistry* **2000**, *39*, 12543–12551.
[28] G. Kopitar, M. Dolinar, B. Štrukelj, J. Pungerčar, V. Turk, *Eur. J. Biochem.* **1996**, *236*, 558–562.
[29] T. A. Pauly, T. Sulea, M. Ammirati, J. Sivaraman, D. E. Danley, M. C. Griffor, A. V. Kamath, I. K. Wang, E. R. Laird, A. P. Seddon, R. Ménard, M. Cygler, V. L. Rath, *Biochemistry* **2003**, *42*, 3203–3213.
[30] J. Y. Gauthier, W. C. Black, I. Courchesne, W. Cromlish, S. Desmarais, R. Houle, S. Lamontagne, C. S. Li, F. Massé, D. J. McKay, M. Ouellet, J. Robichaud, J. F. Truchon, V. L. Truong, Q. Wang, M. D. Percival, *Bioorg. Med. Chem. Lett.* **2007**, *17*, 4929–4933.
[31] D. C. Tully, H. Liu, A. K. Chatterjee, P. B. Alper, R. Epple, J. A. Williams, M. J. Roberts, D. H. Woodmansee, B. T. Masick, C. Tumanut, J. Li, G. Spraggon, M. Hornsby, J. Chang, T. Tuntland, T. Hollenbeck, P. Gordon, J. L. Harris, D. S. Karanewsky, *Bioorg. Med. Chem. Lett.* **2006**, *16*, 5112–5117.
[32] J. Cai, J. Robinson, S. Belshaw, K. Everett, X. Fradera, M. Van Zeeland, L. Van Berkom, P. Van Rijnsbergen, L. Popplestone, M. Baugh, M. Dempster, J. Bruin, W. Hamilton, E. Kinghorn, P. Westwood, J. Kerr, Z. Rankovic, W. Arbuckle, D. J. Bennett, P. S. Jones, C. Long, I. Martin, J. C. M. Uitdehaag, T. Meulemans, *Bioorg. Med. Chem. Lett.* **2010**, *20*, 6890–6894.
[33] P. K. Jadhav, M. A. Schiffler, K. Gavardinas, E. J. Kim, D. P. Matthews, M. A. Staszak, D. S. Coffey, B. W. Shaw, K. C. Cassidy, R. A. Brier, Y. Zhang, R. M. Christie, W. F. Matter, K. Qing, J. D. Durbin, Y. Wang, G. G. Deng, *ACS Med. Chem. Lett.* **2014**, *5*, 1138–1142.
[34] S. Ahmad, M. I. Siddiqi, *J. Mol. Model.* **2017**, *23*, 92.
[35] Y. D. Ward, D. S. Thomson, L. L. Frye, C. L. Cywin, T. Morwick, M. J. Emmanuel, R. Zindell, D. McNeil, Y. Bekkali, M. Giradot, M. Hrapchak, M. DeTuri, K. Crane, D. White, S. Pav, Y. Wang, M. H. Hao, C. A. Grygon, M. E. Labadia, D. M. Freeman, W. Davidson, J. L. Hopkins, M. L. Brown, D. M. Spero, *J. Med. Chem.* **2002**, *45*, 5471–5482.
[36] A. Lee-Dutra, D. K. Wiener, S. Sun, *Exp. Opin. Therap. Patents* **2011**, *21*, 311–337.
[37] J. J. M. Wiener, S. Sun, R. L. Thurmond, *Curr. Top. Med. Chem.* **2010**, *10*, 717–732.
[38] H. Hilpert, H. Mauser, R. Humm, L. Anselm, H. Kuehne, G. Hartmann, S. Gruener, D. W. Banner, J. Benz, B. Gsell, A. Kuglstatter, M. Stihle, R. Thoma, R. A. Sanchez, H. Iding, B. Wirz, W. Haap, *J. Med. Chem.* **2013**, *56*, 9789–9801.
[39] R. D. A. Wilkinson, A. Young, R. E. Burden, R. Williams, C. J. Scott, *Mol. Cancer* **2016**, *15*, 1–11.
[40] J. K. Kerns, H. Nie, W. Bondinell, K. L. Widdowson, D. S. Yamashita, A. Rahman, P. L. Podolin, D. C. Carpenter, Q. Jin, B. Riflade, X. Dong, N. Nevins, P. M. Keller, L. Mitchell, T. Tomaszek, *Bioorg. Med. Chem. Lett.* **2011**, *21*, 4409–4415.
[41] H. A. Katsuhisa Kitano, S. Hamaguchi, *(12) Patent Application Publication (10) Pub. No.: US 2010/0292345 A1 Patent Application Publication*, **2010**.
[42] R. A. Bauer, *Drug Discovery Today* **2015**, *20*, 1061–1073.
[43] A. S. Kalgutkar, D. K. Dalvie, *Expert Opin. Drug Discovery* **2012**, *7*, 561–581.
[44] C. Lammert, S. Einarsson, C. Saha, A. Niklasson, E. Bjornsson, N. Chalasani, *Hepatology* **2008**, *47*, 2003–2009.
[45] T. Schirmeister, J. Kesselring, S. Jung, T. H. Schneider, A. Weickert, J. Becker, W. Lee, D. Bamberger, P. R. Wich, U. Distler, S. Tenzer, P. Johé, U. A. Hellmich, B. Engels, *J. Am. Chem. Soc.* **2016**, *138*, 8332–8335.
[46] C. U. Lee, T. N. Grossmann, *Angew. Chem. Int. Ed.* **2012**, *51*, 8699–8700.
[47] R. A. Copeland, D. L. Pompliano, T. D. Meek, *Nat. Rev. Drug Discovery* **2006**, *5*, 730–739.
[48] J. M. Bradshaw, J. M. McFarland, V. O. Paavilainen, A. Bisconte, D. Tam, V. T. Phan, S. Romanov, D. Finkle, J. Shu, V. Patel, T. Ton, X. Li, D. G. Loughhead, P. A. Nunn, D. E. Karr, M. E. Gerritsen, J. O. Funk, T. D. Owens, E. Verner, K. A. Brameld, R. J. Hill, D. M. Goldstein, J. Taunton, *Nat. Chem. Biol.* **2015**, *11*, 525–531.
[49] S. Jung, N. Fuchs, P. Johe, A. Wagner, E. Diehl, T. Yuliani, C. Zimmer, F. Barthels, R. A. Zimmermann, P. Klein, W. Waigel, J. Meyr, T. Opatz, S. Tenzer, U. Distler, H. J. Räder, C. Kersten, B. Engels, U. A. Hellmich, J. Klein, T. Schirmeister, *J. Med. Chem.* **2021**, *64*, 12322–12358.
[50] D. Brömme, *Curr. Protoc. Protein Sci.* **2000**, *21*, 21.2.1–21.2.14.
[51] C. Yung-Chi, W. H. Prusoff, *Biochem. Pharmacol.* **1973**, *22*, 3099–3108.
[52] D. L. Purich, *Enzyme Kinetics, Catalysis and Control, A Reference of Theory and Best-Practice Methods*, Elsevier, **2010**.
[53] I. D. Kerr, J. H. Lee, C. J. Farady, R. Marion, M. Rickert, M. Sajid, K. C. Pandey, C. R. Caffrey, J. Legac, E. Hansell, J. H. Mckerrow, C. S. Craik, P. J. Rosenthal, L. S. Brinen, *J. Biol. Chem.* **2009**, *284*, 25697–25703.
[54] C. L. Wilder, C. Walton, V. Watson, F. A. A. Stewart, J. Johnson, S. R. Peyton, C. K. Payne, V. Odero-Marah, M. O. Platt, *Int. J. Biochem. Cell Biol.* **2016**, *79*, 199–208.

[55] H. M. Berman, J. Westbrook, Z. Feng, G. Gilliland, T. N. Bhat, H. Weissig, I. N. Shindyalov, P. E. Bourne, *Nucleic Acids Res.* **2000**, *28*, 235–242.
[56] L. Schrödinger, W. DeLano, The PyMOL Molecular Graphics System. Schrödinger, LLC. **2020**. http://www.pymol.org/pymol.
[57] Molecular Operating Environment (MOE). Chemical Computing Group ULC: 1010 Sherbrooke St. West, Suite #910, Montreal, QC, Canada, H3 A 2R7 **2020**.
[58] T. A. Halgren, *J. Comput. Chem.* **1999**, *20*, 720–729.
[59] LeadIT. BioSolveIT GmbH: Sankt Augustin, Germany **2017**. www.biosolveit.de/LeadIT.
[60] I. Reulecke, G. Lange, J. Albrecht, R. Klein, M. Rarey, *ChemMedChem* **2008**, *3*, 885–897.
[61] GraFit. Erithracus Software Ltd.: UK **2006**.

Manuscript received: March 21, 2023
Revised manuscript received: May 18, 2023
Accepted manuscript online: May 24, 2023
Version of record online: June 1, 2023